This manuscript has been accepted for publication in **Cancer Research** (2021) 81 (11): 2874–2887, which is published by the American Association for Cancer Research https://doi.org/10.1158/0008-5472.CAN-20-2052

E2F1 and E2F2-mediated repression of CPT2 establishes a lipid-rich tumor-promoting environment

Francisco González-Romero[1,#], Daniela Mestre[1,2,#], Igor Aurrekoetxea[1,2], Colm J. O´Rourke[3], Jesper B. Andersen[3], Ashwin Woodhoo[4,5], Miguel Tamayo-Caro[4], Marta Varela-Rey[6], Marta Palomo-Irigoyen[4], Beatriz Gómez-Santos[1], Diego Sáenz de Urturi[1], Maitane Núñez-García[1], Juan L. García-Rodríguez[1], Larraitz Fernández-Ares[1,2], Xabier Buqué[1,2], Ainhoa Iglesias-Ara[7], Irantzu Bernales[8], Virginia Gutierrez De Juan[6], Teresa C. Delgado[6], Naroa Goikoetxea-Usandizaga[6], Richard Lee[9], Sanjay Bhanot[9], Igotz Delgado[1], Maria J. Perugorria[10,11], Gaizka Errazti[2], Lorena Mosteiro[2], Sonia Gaztambide[2,12], Idoia Martinez de la Piscina[2], Paula Iruzubieta[13], Javier Crespo[13], Jesus M. Banales[5,10], Maria L. Martínez-Chantar[6], Luis Castaño[2,12], Ana M. Zubiaga[7], Patricia Aspichueta[1,2,*]

[1]Department of Physiology, Faculty of Medicine and Nursing, University of Basque Country UPV/EHU, Leioa, Spain; [2]BioCruces Bizkaia Health Research Institute, Cruces University Hospital, CIBERehd, Barakaldo, Spain; [3]Biotech Research & Innovation Centre, Department of Health and Medical Sciences, University of Copenhagen, Denmark; [4]Center for Cooperative Research in Bioscience (CIC bioGUNE), Derio, Spain. [5]Ikerbasque, Basque Foundation for Science, Bilbao, Spain; [6]Liver Disease Laboratory, Center for Cooperative Research in Biosciences (CIC bioGUNE), Basque Research and Technology Alliance (BRTA), CIBERehd Derio, Spain; [7]Department of Genetic, Physical Anthropology and Animal Physiology, Faculty of Science and Technology, University of Basque Country UPV/EHU, Leioa, Spain; [8]SGIKER, University of Basque Country UPV/EHU, Leioa, Spain; [9]Ionis Pharmaceuticals, California, USA; [10]Department of Liver and Gastrointestinal Diseases, Biodonostia Health Research Institute, Donostia University Hospital, University of the Basque Country UPV/EHU, CIBERehd, San Sebastian, Spain; [11]Department of Medicine, Faculty of Medicine and Nursing, University of the Basque Country UPV/EHU, Leioa, Spain; [12]Faculty of Medicine and Nursing, University of

Basque Country UPV/EHU, CIBERDEM, CIBERER; [13]Gastroenterology and Hepatology Department. Marqués de Valdecilla University Hospital. Santander, Spain.

[#]These authors contributed equally

***Corresponding author**: Patricia Aspichueta, Department of Physiology, Faculty of Medicine and Nursing, University of the Basque Country UPV/EHU, Barrio Sarriena s/n, 48940 Leioa, Spain. Phone: +34 946012896; Fax: +34 946015662; e-mail: patricia.aspichueta@ehu.eus

Running title: E2F1 and E2F2 promote NAFLD-related HCC

Keywords: CPT2/E2F/fatty acid oxidation/lipids/nonalcoholic fatty liver disease/hepatocarcinogenesis

Conflict of Interest: MLM-C is consultant of Mitotherapeutix. JMB reports grants from Incyte, personal fees for lecturer from Bayer and Intercept, and consulting for QED Therapeutics, Albireo Pharma and OWL Metabolomics, outside the submitted work. There are no other conflicts of interest.

Electronic word count without title page, abstract, significant statement, figure legends, acknowledgments and authors contribution: 5,765

Abstract

Lipid metabolism rearrangements in nonalcoholic fatty-liver disease (NAFLD) contribute to disease progression. NAFLD has emerged as a major risk for hepatocarcinogenesis (HCC), where metabolic reprogramming is a hallmark. Identification of metabolic drivers might reveal therapeutic targets to improve HCC treatment. Here, we investigated the contribution of transcription factors E2F1 and E2F2 to NAFLD-related HCC and their involvemnent in metabolic rewiring during disease progression. In mice receiving a high-fat diet (HFD) and diethylnitrosamine (DEN) administration, *E2f1* and *E2f2* expression was increased in NAFLD-related HCC. In human NAFLD, E2F1 and E2F2 levels were increased and positively correlated. *E2f1*$^{-/-}$ and *E2f2*$^{-/-}$ mice were resistant to DEN-HFD-induced hepatocarcinogenesis and associated lipid accumulation. Administration of DEN-HFD in *E2f1*$^{-/-}$ and *E2f2*$^{-/-}$ mice enhanced fatty-acid oxidation (FAO) and increased expression of *Cpt2*, an enzyme essential for FAO whose downregulation is linked to NAFLD-related hepatocarcinogenesis. These results were recapitulated following *E2f2* knockdown in liver, and overexpression of *E2f2* elicited opposing effects. E2F2 binding to the *Cpt2* promoter was enhanced in DEN-HFD-administered mouse livers compared to controls, implying a direct role for E2F2 in transcriptional repression. In human HCC, *E2F1* and *E2F2* expression inversely correlated with *CPT2* expression. Collectively, these results indicate that activation of the E2F1-E2F2-Cpt2 axis provides a lipid-rich environment required for hepatocarcinogenesis.

Electronic word count: 207/250

Statement of significance

Findings identify E2F1 and E2F2 transcription factors as metabolic drivers of hepatocellular carcinoma, where deletion of just one is sufficient to prevent disease.

Introduction

Hepatocellular carcinoma (HCC) is the most common primary liver cancer (1), being the fifth most frequent malignancy in men and the seventh in women globally (2). During the last decade, nonalcoholic fatty liver disease (NAFLD), which affects ~80% of obese patients, has emerged as as an important risk factor for cancer, including HCC (3). The therapeutic options for HCC are still very limited (4) and there is no specific pharmacological treatment for NAFLD. NAFLD-driven HCC has been associated with shorter survival time and more advanced tumor stage (5).

NAFLD begins with the simple storage of lipids within hepatocytes, which may progress to hepatocellular ballooning and cell death, as well as to inflammation, leading to the development of steatohepatitis (nonalcoholic steatohepatitis, NASH). Mechanisms involved in NAFLD progression are still not fully understood. However, lipotoxicity derived from the accumulation of certain lipids may induce inflammation and endoplasmic reticulum stress (6), both processes involved in obesity-driven HCC (7).

A shared feature of HCC and NAFLD is the reprogramming in lipid metabolism. In cancer cells, lipids are required as membrane components, signaling molecules and energy storage, which allow their growth and proliferation. Many lipids are synthesized from acetyl-CoA and/or the derived fatty acids (FA). The relevance of FA biosynthesis for cancer cell growth and survival is well established (8). In HCC, in addition to the *de novo* synthesis of FAs (9), exogenous FAs also support the growth of HCC cells (10). The relevance of lipid catabolism in cancer cells is less clear. In obesity-driven HCC, fatty acid oxidation (FAO) is decreased as the result of the carnitine palmitoyltransferase 2 (CPT2) downregulation, which contributes to carcinogenesis (11). Overall, it is well established that the metabolic switch for malignant cell transformation requires the coordinated modulation of several enzymes and transporters to ensure aberrant proliferation (12). Therefore, the search for pivotal master regulators of lipid metabolism may provide new insights into the mechanisms of liver pathogenesis and novel targets for therapy.

Cell cycle regulators play a dual role triggering proliferation and adapting metabolism in response to external stimuli (13). Some of them have also been described as modulators of

metabolism in non-proliferative cells such as p53, whose deficiency is associated with hepatosteatosis (14) or E2F1 (15-17), the most studied factor of the E2F family.

Here, we investigated the contribution of the cell cycle regulator E2F2 to NAFLD-related HCC by using *in vitro* and *in vivo* models, as well as human samples. Metabolic fluxes, chromatin immunoprecipitation and transcriptomic analyses were performed. Our study unveils a critical function for E2F2 in the regulation of key metabolic enzymes that mediate NAFLD-related hepatocarcinogenesis. Furthermore, we show that the regulation of this metabolic pathway is shared with E2F1, arguing for both E2F1 and E2F2 factors as novel putative therapeutic targets in NAFLD-related liver cancer.

Materials and Methods

Human samples

In this study 78 liver samples were included: non-obese healthy human liver samples (NL) (n=18) from donors (Marqués de Valdecilla University Hospital, Santander, Spain) and liver samples from obese patients (n=60) (Table S1) who underwent a liver biopsy with a diagnostic purpose (Cruces University Hospital, Barakaldo, Spain). NAFLD was diagnosed according to Kleiner's criteria (18). Written consent was obtained from each patient included in the study. This research project was performed in agreement with the Declaration of Helsinki and with local and national laws. The Human Ethics Committee of each hospital and the University of Basque Country approved the study procedures and a written informed consent was obtained before inclusion in the study.

E2F1 and *E2F2* expression analysis in TGCA-LIHC database

Level 3 RNA-seq and clinical datasets generated by TCGA-LIHC project were downloaded from Firehose portal (Broad Institute). In total, 371 tumors and 50 surrounding normal tissues were analyzed). For correlation studies, data normality of genes expression values was assessed by D'Agostino & Pearson normality test. Subsequently, matched expression levels were evaluated by Spearman correlation.

Animal models

Male *E2f1* knockout (*E2f1*$^{-/-}$), *E2f2* knockout (*E2f2*$^{-/-}$), *E2f1*/*E2f2* double knockout (DKO) and their respective wild type (WT) littermate control mice (mixed background C57BL/6J and 129/Sv) were produced at the UPV/EHU animal facility. C57BL/6J mice (Jackson Laboratory, USA) were used for *E2f2* knockdown or overexpression in the liver. Animal procedures were approved by the Ethics Committee for Animal Welfare of the University of the Basque Country UPV/EHU, in accordance with the European Union Directives for animal experimentation.

HCC, with or without NAFLD background, was induced by an intraperitoneal injection of the hepatic carcinogen diethylnitrosamine (DEN) (25 mg/kg of mice, Sigma-Aldrich, USA) in 14 day-old *E2f1*$^{-/-}$ or *E2f2*$^{-/-}$, and WT mice (7). One month after weaning, mice were fed a high fat diet (HFD) (DEN-HFD) or a chow diet (CD) (DEN-CD) for either 32 weeks and sacrificed at 9 months of age (HCC or NAFLD-related HCC model) or for 10 weeks and sacrificed at 3 months of age (NAFLD model). A group of mice fed with HFD or CD alone was also included.

Liver-specific *E2f2* knockdown or overexpression was performed in C57BL/6J mice through the injection of recombinant adeno-associated viruses, serotype 8 (AAV8-shE2F2/AAV8-shScramble for knockdown and AAV8-*E2f2*/AAV8-*GfP* for overexpression), diluted in saline buffer. The *in vivo Creb* downregulation was performed with antisense oligonucleotides (ASO). For this, DEN-HFD *E2f2*$^{-/-}$ and DEN-HFD WT mice received an injection of ASO CREB or ASO control (Ionis Pharmaceuticals, USA).

Statistical analysis

Data are represented as mean ± SEM. Differences between groups were analyzed with Student's t test. Significance was defined as $p<0.05$. For correlation studies in human samples, data normality was assessed by D'Agostino & Pearson normality test. Subsequently, matched gene expression levels were evaluated by Spearman correlation. See figure legends for more details.

Data availability

The datasets and computer code produced in this study are available in the following databases:

— RNA-seq data: Gene expression Omnibus **GSE117420**

Additional methods are described in supplementary material.

Tables with the sequences of oligonucleotides (Table S2) and the dilutions and references of antibodies (Table S3) are included in the supplementary material.

Results

E2F2 promotes hepatocarcinogenesis

Expression of *E2F2* in human HCC was analyzed using the TCGA-LIHC cohort (19). We found that *E2F2* is upregulated in HCC tissue compared to the surrounding normal liver (SL) and that, in general, its expression increases with tumor and disease stage (Fig. S1A), consistent with previous reports (20,21). We next evaluated whether E2F2 is required for HCC development. For this purpose, HCC tumors were induced in WT and *E2f2*$^{-/-}$ mice through the administration of DEN followed by a long-term HFD feeding regimen (a well-established NAFLD-driven HCC model) for 32 weeks (Fig. S1B) (7). Similar to our observations in human HCC, the expression of *E2f2* was found upregulated in mouse HCC tumors compared to normal liver tissue (Fig. 1A). Strikingly, *E2f2*$^{-/-}$ mice (Fig. S1C) were protected against hepatocarcinogenesis, as a nearly complete reduction of liver tumors induced by HFD, by DEN or by DEN-HFD was observed in these mice compared to controls (Fig. 1B). Moreover, liver to body weight ratio, serum alanine aminotransferase (ALT) levels (Fig. 1C) and a reduced expression of several E2F target genes involved in cell cycle progression (Fig. S1D; Fig. S1E) confirmed the protective features of *E2f2*$^{-/-}$ mice to NAFLD-driven HCC development.

Metabolic rearrangements in *E2f2*$^{-/-}$ mice confer protection against hepatocarcinogenesis by preventing lipid storage

A hallmark of NAFLD-related HCC is the lipid accumulation inside tumor hepatocytes (22). Remarkably, the increased storage of triglycerides (TG) and cholesteryl esters (CE) observed in NAFLD-driven HCC samples from WT mice was totally prevented in *E2f2*$^{-/-}$ mice (Fig. 2A). Furthermore, the lipid droplets found in livers of DEN-HFD WT mice, which are mainly located within tumor hepatocytes, were absent in similarly treated *E2f2*$^{-/-}$ mice (Fig. 2B). These data indicate an important role for E2F2 in the regulation of the hepatic lipid metabolism.

We next analyzed the transcriptome that underlies the resistance to develop HCC in DEN-HFD treated *E2f2*$^{-/-}$ mice. The most significantly upregulated pathway within the *E2f2*$^{-/-}$ mice

compared to WT was that concerning to “metabolism”, which included genes related to lipid catabolism (Fig 2C). Among the downregulated genes, the most significantly altered pathways were “Immune system”, “Signaling by Rho GTPases” and “Platelet activation, signaling and aggregation” (Fig. S2A), which are linked to HCC development, as described recently (23). For the validation of these results, we selected genes involved lipid oxidation (Fig. 2D and Fig. S2B) and oxidative phosphorylation (Fig. S2B). The expression of several key genes involved in fatty acid β-oxidation (FAO), typically downregulated in NAFLD-driven HCC in WT mice, were increased in DEN-HFD *E2f2*$^{-/-}$ mice (Fig. 2D and Fig. S2B) together with an elevated FAO rate (Fig. 2E). Similar results were obtained when we compared FAO rates and the mRNA expression levels between *E2f2*$^{-/-}$ and WT mice fed HFD alone (Fig. S2C and Fig. S2D). In concordance, a comparison of the expression levels of genes involved in cell cycle, lipid oxidation and oxidative phosphorylation in CD, HFD and DEN-HFD treated *E2f2*$^{-/-}$ and WT mice showed that *E2f2* deficiency results in changes with the same trend in the DEN-HFD and the HFD group (Fig. S2E)

In line with these findings, *E2F2* knockdown (si*E2F2*) in cycling HepG2 cancer cells (Fig. S3A) reduced significantly lipid droplet accumulation (BODIPY staining) and cellular TG levels (Fig. 2F), and increased FAO rate (Fig. 2G), features that resemble those observed in the *E2f2*$^{-/-}$ mouse livers resistant to HCC. Concomitant to the extensive changes in metabolism, acute E2F2 silencing in HepG2 cells had a subtle effect in the cell cycle, as shown by the approximately 5% reduction in S/G2/M cells compared to siControl (Fig. 2H). Overexpression of *E2F2* (p*E2F2*) in cycling HepG2 cells (Fig. S3A) led to a decreased FAO rate (Fig. S3B) together with a modest induction of E2F target gene expression and cell cycle progression (Fig. S3C). Finally, we overexpressed E2F2 *in vivo* in non-cycling mouse liver cells through the injection of recombinant AAV8-*E2f2* to healthy mice (Fig. S3D). Sustained liver *E2f2* overexpression promoted a substantial reduction in FAO rate when compared to control AAV8-*GfP* mice (Fig. S3E) without inducing significant changes in cell cycle gene expression (Fig. S3F). The results suggest that E2F2 is a prominent regulator of lipid metabolism in cancer and healthy liver cells. Interestingly, this novel role of E2F2 appears to be independent of its classical role in cell cycle regulation.

E2F2 deficiency in mice prevents nonalcoholic fatty liver disease

We next investigated whether E2F2 could also play a metabolic role in the onset of NAFLD. For this, a short-term HFD-induced carcinogenic protocol was used (Fig. S1B) whereby mice were sacrificed at an earlier time (3 *vs* 9 months of age), prior to tumor development and to induction of cell cycle gene expression and Ki67 (Fig. S4A and Fig. S4B). A group of mice that received the HFD alone was also included. Upon short-term HFD or DEN-HFD exposure, *E2f2*$^{-/-}$ mice were resistant to the TG accumulation (Fig. 3A) and lipid droplet storage (Fig. 3B), and maintained lower levels of liver CE than their corresponding WT mice (Fig. 3A). The DEN-HFD mediated increase in ALT values was totally prevented in *E2f2*$^{-/-}$ mice, in which the liver to body weight was decreased (Fig. S4C). The initiation of inflammation (Fig. S4D) and the activation of endoplasmic reticulum stress (Fig. S4E), usually linked with NAFLD progression, were also attenuated in *E2f2*$^{-/-}$ mice compared to the corresponding WT mice, as shown by the expression of *Il1-β* and the phosphorylation of eIF2-α, respectively. Among all the genes involved in FAO and oxidative phosphorylation that were found upregulated in *E2f2*$^{-/-}$ mice under long-term DEN-HFD exposure, only the expression of *Ppargc1a*, *Cpt2* and *Acsl1* was increased after a short-term administration (Fig. 3C, Fig.S5A and Fig. S5B). When mice were fed the HFD alone, mRNA levels of *Cpt2* and *Ppargc1a* were also increased; however, those of *Acsl1* (Fig. S5C), and of some genes involved in oxidative phosphorylation were decreased (Fig. S5D). The FAO rate was already elevated in short-term DEN-HFD *E2f2*$^{-/-}$ mice (Fig. 3D) and in mice fed the HFD alone (Fig. S5E) to levels that were similar to those found after a long-term exposure. These changes in FAO rate were not linked to changes in TOM20 protein levels, a marker of mitochondria (24,25), or in PGC1α, involved in mitochondrial biogenesis (26) (Fig. 3E). A significant upregulation in FAO rate was also observed in primary hepatocytes isolated from DEN-HFD *E2f2*$^{-/-}$ mice compared to their WT counterparts (Fig. 3F), which was coupled to increased mitochondrial oxygen consumption rate (OCR) (Fig. 3G). This was not observed in CD fed *E2f2*$^{-/-}$ hepatocytes (Figure S5F).

E2F1, an E2F family member closely related to E2F2, plays an essential role in regulation of glycolysis in liver, a process that provides compounds required for the *de novo* lipogenesis (17). Given the relevance of glycolysis in NAFLD and HCC, we measured the extracellular acidification rate (ECAR) upon glucose injection into a Seahorse analyser, as a readout of glycolysis, in primary hepatocytes isolated from CD and DEN-HFD *E2f2*$^{-/-}$ and the corresponding WT mice. While glycolysis was decreased in *E2f2*$^{-/-}$ hepatocytes from CD fed mice when compared to the corresponding WT hepatocytes (Fig. S6A), it remained unaltered in *E2f2*$^{-/-}$ hepatocytes from DEN-HFD mice (Fig. S6B). The expression of glucokinase (*Gck*) was downregulated in CD and DEN-HFD *E2f2*$^{-/-}$ hepatocytes while that of piruvate kinase (*Plkr*) remained unaltered (Fig. S6C).

One of the mechanisms involved in the generation of hepatosteatosis is the *de novo* lipogenesis. E2F1 promotes *de novo* fatty acid synthesis through modulation of *Acaca* and *Fasn* expression (17). Thus, we analyzed in *E2f2*$^{-/-}$ mice the expression of genes involved in *de novo* lipogenesis. The levels of malonyl-CoA, the product of the rate limiting reaction in the *de novo* lipogenesis and an inhibitor of FAO, and the metabolic flux that regulates *de novo* synthesis of TG from ^{3}H-acetate were also examined. Expression of *Acaca* and *Fasn* genes was increased in untreated CD *E2f2*$^{-/-}$ mouse livers when compared to corresponding normal controls (Fig. S6D). However, their expression (Fig. S6D), as well as the liver concentration of malonyl-CoA (Fig. S6E) and *de novo* lipogenesis of TG from acetate (Fig. S6F), were unchanged in DEN-HFD *E2f2*$^{-/-}$, indicating that this pathway is not involved in E2F2-mediated remodeling of lipid metabolism.

Another mechanism involved in lipid storage in NAFLD is the dysregulated VLDL secretion (27). However, the hepatic expression (mRNA) of *Apob* or *Apoe* (Fig. S6G), required for VLDL assembly, and the *in vivo* hepatic TG secretion rate did not change in *E2f2*$^{-/-}$ DEN-HFD mice (Fig. S6H). Mice fed with HFD alone showed similar results, except for an increased expression of *Apob* mRNA (Fig. S7A-D). Altogether, these results indicate that the increased FAO rate is the main mechanism involved in the resistance that *E2f2*$^{-/-}$ mice exhibit to lipid storage upon NAFLD induction.

E2F2 represses FAO in the liver by targeting *Cpt2*

Among the genes involved in FAO, *Cpt2* was consistently upregulated in both short-term and long-term DEN-HFD treated *E2f2*$^{-/-}$ mice, as well as in CD *E2f2*$^{-/-}$ mice as compared to their WT counterparts (Fig. 3C). To validate our results in another setting, liver-specific knockdown of *E2f2* was performed in CD WT mice with AAV8 carrying specific small shRNAs against *E2f2*. In agreement with our results in *E2f2* knockout animals, acute silencing of *E2f2* led to increased CPT2 protein levels and FAO rates (Fig. 4A and Fig. 4B).

Considering the established role for *Cpt2* in the promotion of NAFLD-related HCC (11), we evaluated its potential regulation by E2F2. Indeed, we found that *E2F2* and *CPT2* expression inversely correlate in human HCC (TCGA-LIHC cohort) (Fig. 4C). Building on these results, we evaluated if E2F2 could directly repress *Cpt2* gene expression. The INSECT 2.0 tool revealed the presence of several E2F binding sites in the *Cpt2* gene, including one near the transcription initiation site. Chromatin immunoprecipitation (ChIP) followed by amplification of this region of the *Cpt2* promoter showed an enrichment of E2F2 binding in DEN-HFD WT mice livers compared to CD WT mice (Fig. 4D). In concordance, CPT2 protein levels were increased in DEN-HFD *E2f2*$^{-/-}$ mice compared to their WT controls (Fig. 4E). To assess more directly E2F2 binding activity in primary cells, we performed ChIP analyses after overexpressing *E2f2* in hepatocyte cultures, derived from WT mice, by treatment with adenoviruses carrying the specific plasmid for it (Fig. S8A). Overexpression of *E2f2* induced downregulation in *Cpt2* mRNA levels (Fig. S8B), concomitant with an enrichment of E2F2 in the promoter of *Cpt2* (Fig. S8C). Similarly to what has been described for E2F1 (17), there was also an enrichment of E2F2 in the promoters of several genes involved in glycolysis (Fig. S8D). However, unlike E2F1, we did not find an enrichment of E2F2 in the promoters of genes involved in fatty acid synthesis (Fig. S8C) or a significant enrichment in those involved in mitochondrial activity (Fig. S8E).

Chromatin location and gene expression data collected from DEN-HFD mice and E2F2 overexpressing hepatocytes suggest a role for E2F2 as a direct repressor of liver *Cpt2*. To examine further the mechanism of E2F2-mediated *Cpt2* gene regulation, we assessed the contribution of

pRB, given its well-established role in E2F-mediated target gene repression (16), pRB was downregulated in hepatocytes isolated from DEN-HFD and CD WT mice (Fig. S9A). Contrary to what was expected, downregulation of *Rb* decreased *Cpt2* expression in hepatocytes from DEN-HFD WT mice, while it did not induce changes in hepatocytes from CD WT mice (Fig. S9B). Thus, these results suggest that pRB is not involved in E2F2-mediated *Cpt2* gene repression.

The *Cpt2* gene promoter harbors a CREB binding site near an E2F site (Fig. S9C). Given that E2F2 and CREB cooperate in regulating the expression of some target genes (28) and that CREB is also involved in modulation of lipid metabolism (29) we assessed the contribution of CREB to *Cpt2* gene regulation. In DEN-HFD WT mice, *in vivo* administration of CREB1 antisense oligonucleotides (ASO) lowered liver CPT2 protein levels and FAO rate (Fig. S9D). By contrast, in DEN-HFD *E2f2*$^{-/-}$ mice, reduced CREB1 levels had no effect in CPT2 levels or FAO rate (Fig. S9E). These results suggest that CREB1 modulates E2F2-mediated *Cpt2* repression and subsequent FAO reactions.

E2f1 deficiency leads to *Cpt2* upregulation and prevents NAFLD-related hepatocarcinogenesis

E2F1 induces the expression of lipogenic genes, contributing to hepatosteatosis (17) and its overexpression promotes hepatocarcinogenesis (30). However, it is unknown whether E2F1 regulates hepatic FAO in NAFLD-related HCC.

Our data confirm that *E2F1* is upregulated in human HCC tissue compared to the surrounding normal liver (SL) (Fig. S10A) within the TCGA-LIHC cohort, consistent with previous reports (20,21). Accordingly, *E2f1* levels were increased in mouse livers with NAFLD-related HCC (DEN-HFD) (Fig. 5A), and *E2f1*$^{-/-}$ mice showed protection against NAFLD-related HCC development (Fig. 5B). Consistently, DEN-HFD *E2f1*$^{-/-}$ mice were also resistant to liver TG storage (Fig. 5C). Following these results, we investigated the degree of similarity between the transcriptome hallmark that underlies the protection against NAFLD-related HCC in *E2f1*$^{-/-}$ and

E2f2$^{-/-}$ mice. The most significantly changed pathways within the upregulated genes in DEN-HFD *E2f1*$^{-/-}$ mice compared with the DEN-HFD WT controls were those related to metabolism of lipids and fatty acids (Fig S10B), and among the downregulated genes were those related to "immune system" and "platelet activation, signaling and aggregation" (Fig. S10C). The analysis of genes commonly upregulated between DEN-HFD *E2f1*$^{-/-}$ and DEN-HFD *E2f2*$^{-/-}$ mice showed 704 genes (Fig. 5D), most of them related to metabolic pathways and some to fatty acid metabolism (Fig. 5E).

The genes related to FAO and oxidative phosphorylation that were upregulated in DEN-HFD *E2f2*$^{-/-}$ mice (Fig. 2C and Fig. S2B), were also found upregulated in DEN-HFD *E2f1*$^{-/-}$ mice (Fig. 5F, Fig. S10D and Fig. S10E), including *Cpt2* (Fig. 5F) together with the FAO rate (Fig. 5G). Moreover, *E2F1* and *CPT2* correlated negatively in human HCC (TCGA-LIHC cohort) (Fig. 5H) and *Cpt2* was upregulated in 3 month-old CD fed *E2f1*$^{-/-}$ mice (Fig. 5I). This effect was not the result of a cross-regulation between *E2f1* and *E2f2*, because livers of *E2f1/E2f2* double knockout (DKO) mice fed a CD exhibited levels of *Cpt2* expression that were practically the sum of those found in single knockout mice (Fig 5I). Moreover, during disease progression, expression of *E2f1* was decreased in the *E2f2*$^{-/-}$ mice as compared to their WT mice, implying that *E2f1* does not compensate for the loss of *E2f2* (Fig. S10F and Fig. S10G). Taken together, these results suggest that both E2F1 and E2F2 contribute independently to *Cpt2* gene repression in the liver.

E2F1 and E2F2 protein levels are increased in human NAFLD

E2F1 and *E2F2* expression positively correlated in human HCC from the TCGA-LIHC cohort (Fig. 5J). Given our evidences that E2F1 and E2F2 play a major role as regulators of the FAO rate involved in the development of NAFLD and NAFLD-related hepatocarcinogenesis, we measured E2F1 and E2F2 protein levels in livers from a cohort of obese patients with and without NAFLD (Table S1). A group of non-obese normal liver (NL) patients was also included. E2F2 levels were found increased in the liver of patients with NAFLD compared to NL (Fig. 6A). The same profile was observed for E2F1 protein levels (Fig. 6B). E2F1 and E2F2 levels were higher

in NL from obese patients than in NL from non-obese subjects. Correlation between both proteins was observed in obese patients' livers (Fig. 6C).

Discussion

Altered lipid metabolism is a common feature of most cancers (8). In malignant cells, rewiring of lipid metabolism provides lipids for the synthesis of membranes, activation of signaling cascades and energy storage (31). In the case of liver carcinogenesis this setting is even more complex. The liver controls metabolic homeostasis of the whole body, but when the uptake of dietary lipids is overloaded, such as in obesity, the increased liver lipid input is not compensated by pathways involved in lipid output, thus leading to NAFLD (32). NAFLD, with its rising worldwide prevalence linked with obesity, represents a major risk for HCC development. There is no pharmacological therapies for NAFLD and effective treatments for HCC are required. Therefore, the prevention and/or restoration of the metabolic rewiring associated to NAFLD and HCC represent novel attractive strategies. There is growing evidence of a regulatory axis between cell cycle regulators and metabolic fluxes. Here, we investigated the etiopathogenic role of E2F1 and E2F2 transcription factors in NAFLD and NAFLD-related HCC, and their potential value as targets for therapy in these health conditions.

We show that E2F2 is upregulated in NAFLD and NAFLD-related HCC, and that loss of E2F2 prevents the development of NAFLD and NAFLD-related HCC, implying an oncogenic role for E2F2 in liver hepatocarcinoma, as has been described in other cancer types (33). The requirement of E2F2 for liver regeneration after partial hepatectomy (34), supports its proliferative role in liver. Biological pathways typically upregulated in HCC, such as platelet activation/signaling and cell cycle, were downregulated in *E2f2*$^{-/-}$ mice administered with DEN-HFD, consistent with the protection against HCC development in these mice. Importantly, we have uncovered a novel E2F2-dependent mechanism for liver disease, by demonstrating that E2F2 is a key regulator of lipid metabolism in liver and a driver of liver cancer in a manner that appears to be independent of its cell cycle regulator function. The reprogramming in lipid metabolism is of high relevance in cancer, but the specific metabolic pathways that sustain the supply of energy and/ or other sources for cell survival is a feature to be determined for each cancer type. It will be important to

evaluate to what extent other cancer types rely on E2F2-regulated metabolic pathways to support cancer growth.

E2f2 knockout mouse livers and *E2F2* knockdown HCC cell lines displayed similar metabolic profiles, characterized by decreased TG concentration and increased fatty acid oxidation (FAO) rate. The decreased lipid storage was associated to a transcriptome profile characterized by the upregulation of genes involved in FAO. The relevance of FAO in cancer cells is still not fully understood. Some cancers benefit from FAO (35) whereas others such as NAFLD-related HCC exhibit the opposite response (11). The rate limiting step that controls FAO is the carnitine-acylcarnitine shuttle, where FAs are converted to acylcarnitines through CPT1. In turn, CPT2 will release them as acyl-CoAs into the mitochondrial matrix (36). It has been reported that in NAFLD-related HCC, CPT2 levels are decreased, leading to decreased FAO rate and to the accumulation of acylcarnitines (11). The decrease in FAO rate promotes lipid storage while the accumulation of acylcarnitines promotes the activation of STAT3 and proliferation (11). Increased lipid storage leads to lipotoxicity-induced hepatocyte cell death in some patients promoting progression of NAFLD to NASH and even to HCC (37,38). However, HCC cells need to survive in this lipid-rich environment, and decreased CPT2 expression is associated with resistance of HCC cells to chronic exposure to palmitic acid (11). Thus, the upregulation of CPT2 and FAO, such as what we observe in the absence of E2F2, would prevent lipid accumulation, its associated lipotoxicity and activation of an ER stress response, thereby hindering disease development and progression. So far, the only known regulator of CPT2 is PPARα (39). Here, we demonstrate by using ChIP assays and transcriptomic analyses that E2F2 binds to *Cpt2* promoter and represses its expression, which is consistent with the fact that *E2F2* inversely correlates with *CPT2* in human HCC. The mechanisms by which E2F factors may activate genes involved in cell cycle while repress others involved in metabolism is still unresolved. It has been shown that E2F family can function as direct repressors of transcription through their well-known interaction with pRB (40) or independently via recruitment of corepressors such as BIN1 or KAP1 (41,42). Regarding metabolism genes, it has been reported that pRB is involved in E2F1-mediated

mitochondrial gene repression (16). Conversely, our study shows that E2F2-mediated *Cpt2* gene repression in DEN- HFD treated or CD fed mice is independent of pRB. The identification of putative E2F2 co-repressors involved in *Cpt2* repression remains to be addressed in future studies.

E2F2 shares with E2F1 multiple target genes and cellular functions, but there is also target specificity (43). In the liver, increased E2F1 and E2F2 levels positively correlate in human HCC and in human NAFLD, suggesting that regulation of these two factors in liver disease might respond to the same effectors. A role for E2F1 in hepatocarcinogenesis has been previously reported, associated with an upregulated expression of E2F target genes involved mainly in cell cycle and DNA repair (30). We now identify a novel regulatory pathway by which both E2F1 and E2F2 contribute to NAFLD-related HCC development in mice, through a mechanism that involves *Cpt2* gene repression, FAO and mitochondrial activity. Of relevance, the upregulated levels of *Cpt2* in *E2f1/E2f2* DKO mice were higher that the levels found in *E2f1*$^{-/-}$ and *E2f2*$^{-/-}$ mice, revealing a new overlapping role of E2F1 and E2F2 in the repression of *Cpt2* in NAFLD-related HCC. However, the lack of either *E2f1* or *E2f2* is enough to protect from NAFLD and NAFLD-related hepatocarcinogenesis. This is an important issue given that the concomitant lack of both E2F1 and E2F2, and subsequent overexpression of CPT2, would induce FAO to a level that may generate ROS without resolving liver disease (44). However, supporting the fact that E2F1 and E2F2 also regulate different target genes, our results here show that *Acaca* and *Fasn* expression and *de novo* lipogenesis of TG from acetate are not regulated by E2F2, in contrast to what has been described for E2F1 (17).

In sum, our data demonstrate that both E2F1 and E2F2 repress CPT2 expression, leading to the generation of a lipid-rich environment required for hepatocarcinogenesis (Figure 7). However, of note, the lack of just one of them is enough to prevent liver disease. These data identify E2F1 and E2F2 as new metabolic drivers that regulate the rewiring of metabolism in NAFLD-related HCC, arising as novel targets for therapy.

Acknowledgements

This work was supported by "Ayudas para apoyar grupos de investigación del sistema Universitario Vasco" (IT971-16 to P.A and IT1257-19 to A.M.Z.), MCIU/AEI/FEDER, UE (SAF2015-64352-R and RTI2018-095134-B-100) (to P.A.), MCIU/AEI/FEDER, UE (SAF2015-67562-R and RTI2018-097497-B-100) (to A.M.Z.), MINECO-FEDER SAF2017-87301-R (to M.L.M-C), MINECO-FEDER EU ("Subprograma Ramon y Cajal" RYC2010-06901) (to A.W.); MINECO-FEDER SAF2015- 65360-R (to A.W.); MINECO-FEDER SAF2015-72416-EXP (to A.W.); MINECO-FEDER SAF2015-62588-ERC (to A.W.), MCIU/AEI/FEDER, UE (RTI2018-097503-B-I00, SEV-2016-0644) (to A.W), European Research Council (Consolidator grant under the EU's Horizon 2020 research and innovation programme; grant agreement 865157) (to A.W.), Gilead Sciences Research Scholars Programs (to M.V.R), Leonardo Grant for Researchers and Cultural Creators BBVA Foundation (to M.V.R) (to A.W) and "Ciberehd Emergente" (to M.V.R), BIOEF (Basque Foundation for Innovation and Health Research): EITB Maratoia (BIO15/CA/014 to M.L.M.-C and BIO15/CA/016 to J.M.B), La Caixa Fundation and "AYUDAS FUNDACIÓN BBVA A EQUIPOS DE INVESTIGACIÓN CIENTÍFICA" 2018 (HR17-00601 to M.L.M.-C and J.M.B). AECC ("Cáncer Infantil"; JP Vizcaya) (to A.W.). J.M.B was funded by the Spanish Carlos III Health Institute (ISCIII) [FIS PI15/01132, PI18/01075 and Miguel Servet Program CON14/00129 and CPII19/00008] cofinanced by "Fondo Europeo de Desarrollo Regional" (FEDER), AMMF-The Cholangiocarcinoma Charity, Euskadi RIS3 (2019222054), and "Fundación Científica de la Asociación Española Contra el Cáncer" (AECC Scientific Foundation; "Rare cancers grant 2017" to J.M. Banales and M.L.M.-C). Ciberehd_ISCIII_MINECO is funded by ISCIII.

The results published here are in part based upon data generated by the TCGA Research Network: https://www.cancer.gov/tcga.

CIC-BioGUNE thanks MINECO for the Severo Ochoa Excellence Accreditation (SEV-2016 0644).

We thank Jose Antonio Lopez from the Department of Physiology, Faculty of Medicine and Nursing UPV/EHU and SGIKER from UPV/EHU

Author Contributions: DM, FG-R and PA designed the project; DM, FG-R, IA, CJOR, JBA, AW, MV-R, XB, IB, VG, RL, SB, AMZ and PA designed experimental protocols; DM, FG-R, IA, CJOR, AW, MV-R, MT-C, MP-I, BG-S, DS, MN-G, JLG-R, LF-A, XB, AI, VG, TCD, NG-U, ID, MJP, GE, LM, SG, IM, PI, JC, JMB, MLM-C, LC, AMZ and PA contributed to investigations and data analysis; DM, FG-R, JMB, AMZ and PA contributed to discussions; DM, FG-R, AMZ and PA wrote the manuscript with input from all the other authors.

References

1. Villanueva A. Hepatocellular carcinoma. *N Engl J Med*. 2019;380(15):1450-1462.

2. El-Serag HB. Epidemiology of viral hepatitis and hepatocellular carcinoma. *Gastroenterology*. 2012;142(6):1264-1273.e1.

3. Younes R, Bugianesi E. Should we undertake surveillance for HCC in patients with NAFLD? *J Hepatol*. 2018;68(2):326-334.

4. Gerbes A, Zoulim F, Tilg H, Dufour J, Bruix J, Paradis V, et al. Gut roundtable meeting paper: Selected recent advances in hepatocellular carcinoma. *Gut*. 2018;67(2):380-388.

5. Younossi ZM, Otgonsuren M, Henry L, Venkatesan C, Mishra A, Erario M, et al. Association of nonalcoholic fatty liver disease (NAFLD) with hepatocellular carcinoma (HCC) in the united states from 2004 to 2009. *Hepatology*. 2015;62(6):1723-1730.

6. Marra F, Svegliati-Baroni G. Lipotoxicity and the gut-liver axis in NASH pathogenesis. *J Hepatol*. 2018;68(2):280-295.

7. Park EJ, Lee JH, Yu G, He G, Ali SR, Holzer RG, et al. Dietary and genetic obesity promote liver inflammation and tumorigenesis by enhancing IL-6 and TNF expression. *Cell*. 2010;140(2):197-208.

8. Currie E, Schulze A, Zechner R, Walther TC, Farese RV. Cellular fatty acid metabolism and cancer. *Cell Metab*. 2013;18(2):153-161.

9. Li L, Pilo GM, Li X, Cigliano A, Latte G, Che L, et al. Inactivation of fatty acid synthase impairs hepatocarcinogenesis driven by AKT in mice and humans. *J Hepatol*. 2016;64(2):333-341.

10. Cao D, Song X, Che L, Li X, Pilo MG, Vidili G, et al. Both de novo synthetized and exogenous fatty acids support the growth of hepatocellular carcinoma cells. *Liver Int*. 2017;37(1):80-89.

11. Fujiwara N, Nakagawa H, Enooku K, Kudo Y, Hayata Y, Nakatsuka T, et al. CPT2 downregulation adapts HCC to lipid-rich environment and promotes carcinogenesis via acylcarnitine accumulation in obesity. *Gut*. 2018;67(8):1493-1504.

12. Snaebjornsson MT, Janaki-Raman S, Schulze A. Greasing the wheels of the cancer machine: The role of lipid metabolism in cancer. *Cell Metabolism*. 2019.

13. Fajas L. Re-thinking cell cycle regulators: The cross-talk with metabolism. *Frontiers in oncology*. 2013;3:4.

14. Porteiro B, Fondevila MF, Buque X, Gonzalez-Rellan MJ, Fernandez U, Mora A, et al. Pharmacological stimulation of p53 with low-dose doxorubicin ameliorates diet-induced nonalcoholic steatosis and steatohepatitis. *Mol Metab*. 2018;8:132-143.

15. Fajas L, Landsberg RL, Huss-Garcia Y, Sardet C, Lees JA, Auwerx J. E2Fs regulate adipocyte differentiation. *Developmental Cell*. 2002;3(1):39-49.

16. Fritz V, Aguilar V, Auwerx J, Lagarrigue S, Fajas L, Clapé C, et al. E2F transcription factor-1 regulates oxidative metabolism. *Nature Cell Biology*. 2011;13(9):1146-1152.

17. Denechaud P, Lopez-Mejia IC, Giralt A, Lai Q, Blanchet E, Delacuisine B, et al. E2F1 mediates sustained lipogenesis and contributes to hepatic steatosis. *Journal of Clinical Investigation*. 2016;126(1):137.

18. Kleiner DE, Brunt EM, Van Natta M, Behling C, Contos MJ, Cummings OW, et al. Design and validation of a histological scoring system for nonalcoholic fatty liver disease. *Hepatology*. 2005;41(6):1313-1321.

19. Comprehensive and integrative genomic characterization of hepatocellular carcinoma. *Cell*. 2017;169(7):1327-1341.e23.

20. Huang Y, Ning G, Chen L, Lian Y, Gu Y, Wang J, et al. Promising diagnostic and prognostic value of E2Fs in human hepatocellular carcinoma. *Cancer Manag Res*. 2019;11:1725-1740.

21. Hong SH, Eun JW, Choi SK, Shen Q, Choi WS, Han J, et al. Epigenetic reader BRD4 inhibition as a therapeutic strategy to suppress E2F2-cell cycle regulation circuit in liver cancer. *Oncotarget*. 2016;7(22):32628-32640.

22. Salomao M, Remotti H, Vaughan R, Siegel AB, Lefkowitch JH, Moreira RK. The steatohepatitic variant of hepatocellular carcinoma and its association with underlying steatohepatitis. *Hum Pathol*. 2012;43(5):737-746.

23. Malehmir M, Pfister D, Gallage S, Szydlowska M, Inverso D, Kotsiliti E, et al. Platelet GPIbα is a mediator and potential interventional target for NASH and subsequent liver cancer. *Nat Med*. 2019;25(4):641-655.

24. Zhang Y, Chen Y, Gucek M, Xu H. The mitochondrial outer membrane protein MDI promotes local protein synthesis and mtDNA replication. *The EMBO journal*. 2016;35(10):1045-1057.

25. Yamamoto H, Itoh N, Kawano S, Yatsukawa Y, Momose T, Makio T, et al. Dual role of the receptor Tom20 in specificity and efficiency of protein import into mitochondria. *Proc Natl Acad Sci U S A*. 2011;108(1):91-96.

26. LeBleu VS, O'Connell JT, Gonzalez Herrera KN, Wikman H, Pantel K, Haigis MC, et al. PGC-1α mediates mitochondrial biogenesis and oxidative phosphorylation in cancer cells to promote metastasis. *Nat Cell Biol*. 2014;16(10):992-15.

27. Cano A, Buqué X, Martínez-Uña M, Aurrekoetxea I, Menor A, García-Rodríguez JL, et al. Methionine adenosyltransferase 1A gene deletion disrupts hepatic very low-density lipoprotein assembly in mice. *Hepatology*. 2011;54(6):1975-1986.

28. Laresgoiti U, Apraiz A, Olea M, Mitxelena J, Osinalde N, Rodriguez JA, et al. E2F2 and CREB cooperatively regulate transcriptional activity of cell cycle genes. *Nucleic Acids Res*. 2013;41(22):10185-10198.

29. Louet J, Hayhurst G, Gonzalez FJ, Girard J, Decaux J. The coactivator PGC-1 is involved in the regulation of the liver carnitine palmitoyltransferase I gene expression by cAMP in combination with HNF4 alpha and cAMP-response element-binding protein (CREB). *J Biol Chem*. 2002;277(41):37991-38000.

30. Kent LN, Bae S, Tsai S, Tang X, Srivastava A, Koivisto C, et al. Dosage-dependent copy number gains in E2f1 and E2f3 drive hepatocellular carcinoma. *CLIN Journal*. 2017;127(3):830-842.

31. Röhrig F, Schulze A. The multifaceted roles of fatty acid synthesis in cancer. *Nat Rev Cancer*. 2016;16(11):732-749.

32. Berlanga A, Guiu-Jurado E, Porras JA, Auguet T. Molecular pathways in non-alcoholic fatty liver disease. *Clin Exp Gastroenterol*. 2014;7:221-239.

33. Chen L, Yu JH, Lu ZH, Zhang W. E2F2 induction in related to cell proliferation and poor prognosis in non-small cell lung carcinoma. *International journal of clinical and experimental pathology*. 2015;8(9):10545-10554.

34. Delgado I, Fresnedo O, Iglesias A, Rueda Y, Syn W, Zubiaga AM, et al. A role for transcription factor E2F2 in hepatocyte proliferation and timely liver regeneration. *Am J Physiol Gastrointest Liver Physiol*. 2011;301(1):20.

35. Ma Y, Temkin SM, Hawkridge AM, Guo C, Wang W, Wang X, et al. Fatty acid oxidation: An emerging facet of metabolic transformation in cancer. *Cancer Lett*. 2018;435:92-100.

36. Aspichueta P. Lipid-rich environment: A key role promoting carcinogenesis in obesity-related non-alcoholic fatty liver disease. *Gut*. 2018;67(8):1376-1377.

37. Machado MV, Diehl AM. Pathogenesis of nonalcoholic steatohepatitis. *Gastroenterology*. 2016;150(8):1769-1777.

38. Nakagawa H, Umemura A, Taniguchi K, Font-Burgada J, Dhar D, Ogata H, et al. ER stress cooperates with hypernutrition to trigger TNF-dependent spontaneous HCC development. *Cancer Cell*. 2014;26(3):331-343.

39. Rakhshandehroo M, Knoch B, Müller M, Kersten S. Peroxisome proliferator-activated receptor alpha target genes. *PPAR Res*. 2010;2010.

40. Aguilar V, Fajas L. Cycling through metabolism. *EMBO molecular medicine*. 2010;2(9):338-48.

41. Folk WP, Kumari A, Iwasaki T, Pyndiah S, Johnson JC, Cassimere EK, et al. Loss of the tumor suppressor BIN1 enables ATM ser/thr kinase activation by the nuclear protein E2F1 and renders cancer cells resistant to cisplatin. *J Biol Chem*. 2019;294(14):5700-5719.

42. Wang C, Rauscher FJ, Cress WD, Chen J. Regulation of E2F1 function by the nuclear corepressor KAP1. *J Biol Chem*. 2007;282(41):29902-29909.

43. Iglesias-Ara A, Zenarruzabeitia O, Fernandez-Rueda J, Sanchez-Tillo E, Field SJ, Celada A, et al. Accelerated DNA replication in E2F1-and E2F2-deficient macrophages leads to induction of the DNA damage response and p21 CIP1-dependent senescence. *Oncogene*. 2010;29(41):5579-5590.

44. García-Ruiz C, Fernández-Checa JC. Mitochondrial oxidative stress and antioxidants balance in fatty liver disease. *Hepatol Commun*. 2018;2(12):1425-1439.

Figure Legends

Figure 1. **E2F2 is required for hepatocellular carcinoma (HCC) development.** Mice were treated for 32 weeks to induce hepatocarcinogenesis and were sacrificed at 9 months of age. (A) Analysis of hepatic *E2f2* mRNA levels (n=6-8 mice per group). (B) Representative photographs from WT and *E2f2*$^{-/-}$ mouse livers (left) and quantification of tumor number and size (right) (n=7-9 mice per group). (C) Liver-to-body weight ratio (n=6-9 mice per group) and ALT levels in liver homogenates (n=6-9 mice per group). Values represent mean ± SEM. Statistical analysis was determined by Student's two-tailed t-test. Significant differences between *E2f2*$^{-/-}$ and WT mice are denoted as *p <0.05, **p <0.01 and ***p <0.001, and differences between DEN-HFD and CD are denoted as $^{\#}$p <0.05, $^{\#\#}$p <0.01 and $^{\#\#\#}$p <0.001. DEN, diethylnitrosamine; CD, chow diet; HFD, high fat diet; ALT, alanine aminotransferase.

Figure 2. **Rewiring of lipid metabolism in *E2f2*$^{-/-}$ mice prevents the lipid-rich environment for NAFLD-related HCC development.** Mice were treated for 32 weeks to induce hepatocarcinogenesis and were sacrificed at 9 months of age. (A) Liver TG and CE quantification after 32 weeks of treatment (n=4-9 mice per group). (B) Representative liver sections stained with H&E. (C) RNA was extracted from *E2f2*$^{-/-}$ and WT liver homogenates and a gene expression microarray analysis was carried out (n=4 mice per group). Differential gene expression between both genotypes was analyzed and significant probes were assigned into pathways with Reactome database. Biological pathways encompassing upregulated genes ($p \leq 0.001$) in DEN-HFD *E2f2*$^{-/-}$ mice vs DEN-HFD WT mice are shown ($-\log_2$ of 0.001 is indicated with a red line). (D) Hepatic mRNA levels of genes involved in lipid oxidation (n=7-8 mice per group). (E) Fatty acid β-oxidation rate was determined in liver homogenates by measuring the amount of [^{14}C]-CO_2 (complete oxidation of [^{14}C]-palmitate) and [^{14}C]-ASM (incomplete oxidation of [^{14}C]-palmitate) (n=4 mice per group). (F) Lipid content analysis in HepG2 cells upon *E2F2* knockdown with siRNAs. Lipids were labelled with Bodipy Green dye and cell nucleus with DAPI. Representative confocal micrographs of cells with or without oleic acid are shown (left). Cell TG content (right)

(n=4-5 per group). (G) Fatty acid oxidation rate was determined in HepG2 cell cultures by measuring the amount of [^{14}C]-CO_2 and [^{14}C]-ASM released by cells (n=4 per group). (H) Cell cycle distribution analysis in HepG2 cells transfected with si*E2F2* compared to siControl transfected cells (n=6). Values represent mean ± SEM. Statistical analysis was determined by Student's two-tailed t-test. Significant differences between *E2f2*$^{-/-}$ and WT mice are denoted as *p <0.05, **p <0.01 and ***p <0.001, and differences between DEN-HFD and CD are denoted as $^{\#}$p <0.05, $^{\#\#}$p <0.01 and $^{\#\#\#}$p <0.001. TG, triglyceride; CE; cholesteryl ester; CD, chow diet; HFD, high fat diet; DEN, diethylnitrosamine; ASM, acid soluble metabolites.

Figure 3. E2F2 deficiency prevents NAFLD through the induction of fatty acid oxidation rate. Mice were treated for 10 weeks to induce NAFLD and were sacrificed at 3 months of age. (A) Liver TG and CE quantification (n=8-9 mice per group). (B) Representative liver sections stained with H&E. (C) Hepatic mRNA levels of genes involved in lipid oxidation (n=7-8 mice per group). (D) Fatty acid β-oxidation (FAO) rate was determined in liver homogenates by measuring the amount of [^{14}C]-CO_2 and [^{14}C]-ASM (n=4 mice per group). (E) Western blot analysis of TOM20 and PGC1α protein levels in livers (n=6-8 mice per group). (F) Fatty acid β-oxidation rate was determined as above in hepatocytes (n=5 per group). (G) Oxygen consumption rate (OCR) in hepatocytes was measured using the Seahorse analyzer (n=11-12 per group). Values represent mean ± SEM. Statistical analysis was determined by Student's two-tailed t-test. Significant differences between *E2f2*$^{-/-}$ and WT mice are denoted as *p <0.05, **p <0.01 and ***p <0.001, and differences between DEN-HFD and CD are denoted as $^{\#}$p <0.05, $^{\#\#}$p <0.01 and $^{\#\#\#}$p <0.001. TG, triglyceride; CE, cholesteryl ester; CD, chow diet; HFD, high fat diet; DEN, diethylnitrosamine; ASM, acid soluble metabolites.

Figure 4. E2F2 represses CPT2 gene expression in the liver. (A) E2F2 and CPT2 protein levels in CD WT mice after liver specific knockdown of *E2f2* using AAV8s (n=6 mice per group). (B) Fatty acid β-oxidation rate was determined in liver, after specific knockdown of *E2f2* using

AAV8s, by measuring the amount of [^{14}C]-CO_2 and [^{14}C]-ASM (n=6 mice per group). (C) Negative correlation between *E2F2* and *CPT2* expression in HCC tumors from human samples (data from the TCGA-LIHC project). Spearman correlation coefficient is shown. (D) Schematic representation of *Cpt2* gene promoter indicating the localization of a consensus E2F motif detected with Insect 2,0 at a 0.88 threshold level. ChIP-q-PCR analyses of E2F2 target gene *Cpt2* in WT (n=8-10 mice per group) and *E2f2*$^{-/-}$ mice (n=3 mice). ChIP assays were performed using anti-E2F2 and anti-IgG (negative control) antibodies. (E) CPT2 protein levels in liver (n=4 mice per group). Values represent mean ± SEM (mouse analyses) or mean ± SD (human analyses). Statistical analysis was determined by Student's two-tailed t-test. Significant differences between *E2f2*$^{-/-}$ and WT mice are denoted as *p <0.05, **p <0.01 and ***p <0.001, and differences between DEN-HFD and CD are denoted as $^{\#}$p <0.05, $^{\#\#}$p <0.01 and $^{\#\#\#}$p <0.001. CD, chow diet; HFD, high fat diet; DEN, diethylnitrosamine; ChIP, chromatin immunoprecipitation; AAV8, adeno associated virus serotype 8; ASM, acid soluble metabolites; RSEM: RNA-seq by expectation maximization.

Figure 5. E2F1 is required for NAFLD-related HCC and it regulates lipid oxidation through a mechanism shared with E2F2. Mice were treated for 32 weeks to induce hepatocarcinogenesis and were sacrificed at 9 months of age. (A) Analysis of hepatic *E2f1* mRNA levels (n=6-8 mice per group). (B) Representative photographs from WT and *E2f1*$^{-/-}$ mouse livers. (C) Liver TG and CE quantification (n=4-6 mice per group). (D) Venn diagram showing the degree of overlap between the number of differentially upregulated genes in DEN-HFD *E2f1*$^{-/-}$ and DEN-HFD *E2f2*$^{-/-}$ mice. (E) RNA was extracted from *E2f1*$^{-/-}$ and WT liver homogenates and a gene expression microarray analysis was carried out (n=4 mice per group). Differential gene expression between *E2f1*$^{-/-}$ or *E2f2*$^{-/-}$ and WT was analyzed and significant probes were assigned into pathways with Reactome database. Biological pathways including common upregulated genes ($p \leq 0.001$) are shown ($-\log_2$ of 0.001 is indicated with a red line). (F) Hepatic mRNA levels of genes involved in lipid oxidation (n=6-8 mice per group). (G) Fatty acid β-oxidation rate was determined in liver

homogenates by measuring the amount of [^{14}C]-CO_2 and [^{14}C]-ASM (n=5 mice per group). (H) Negative correlation between *E2F1* and *CPT2* expression in HCC tumors from human samples (data from the TCGA-LIHC project). (I) Hepatic mRNA levels of *Cpt2 in* WT, *E2f2*$^{-/-}$, *E2f1*$^{-/-}$ and *E2f1*/*E2f2* double knockout (DKO) mice (n=4-5 mice per group). (J) Positive correlation between *E2F1* and *E2F2* expression in HCC tumors from human samples (data from the TCGA-LIHC project). Values represent mean ± SEM (mouse analyses) or mean ± SD (human analyses). Statistical analysis was determined by Student's two-tailed t-test. Significant differences between *E2f2*$^{-/-}$ and WT mice are denoted as *p <0.05, **p <0.01 and ***p <0.001, and differences between DEN-HFD and CD are denoted as $^{\#}$p <0.05, $^{\#\#}$p <0.01 and $^{\#\#\#}$p <0.001. Spearman correlation coefficient is shown. CD, chow diet; HFD, high fat diet; DEN, diethylnitrosamine; TG, triglyceride; CE, cholesteryl ester; ASM, acid soluble metabolites; RSEM: RNA-seq by expectation maximization

Figure 6. E2F1 and E2F2 are increased in human NAFLD. (A) Immunohistochemical analysis of E2F2 in patients (n=78) with NAFLD or NL. (B) Immunohistochemical analysis of E2F1 in patients (n=78) with NAFLD or NL. (C) Correlation analyses between *E2F1* and *E2F2* expression in a human cohort of obese patients with and without NAFLD. A group of non-obese NL patients was also included. Values represent the mean. Differences between NAFLD (obese) or NL (non-obese or obese) are denoted by *p <0.05, **p <0.01 and ***p <0.001 (Student's t test). Spearman correlation coefficient is shown. NL, normal liver; NAFLD, non-alcoholic fatty liver.

Figure 7. Proposed model for the role of E2F2 and E2F1 in the development of NAFLD and progression to HCC. Increased E2F1 and E2F2 activity in liver inhibits CPT2 expression, which would hamper fatty acid oxidation rate from increasing in response to an elevated lipid flux. This metabolic dysregulation would boost a lipid-rich environment with increased acylcarnitine levels, thereby promoting the progression of liver disease, including Kupffer cell activation and the recruitment of platelets. LSEC, liver sinusoidal endothelial cells; L, lymphocyte; P, platelet; N,

neutrophil; KC, Kupffer cells; HSC, hepatic stellate cells; DS, Disse space; FAO, fatty acid oxidation; NAFLD, non-alcoholic fatty liver disease; HCC, hepatocellular carcinoma.

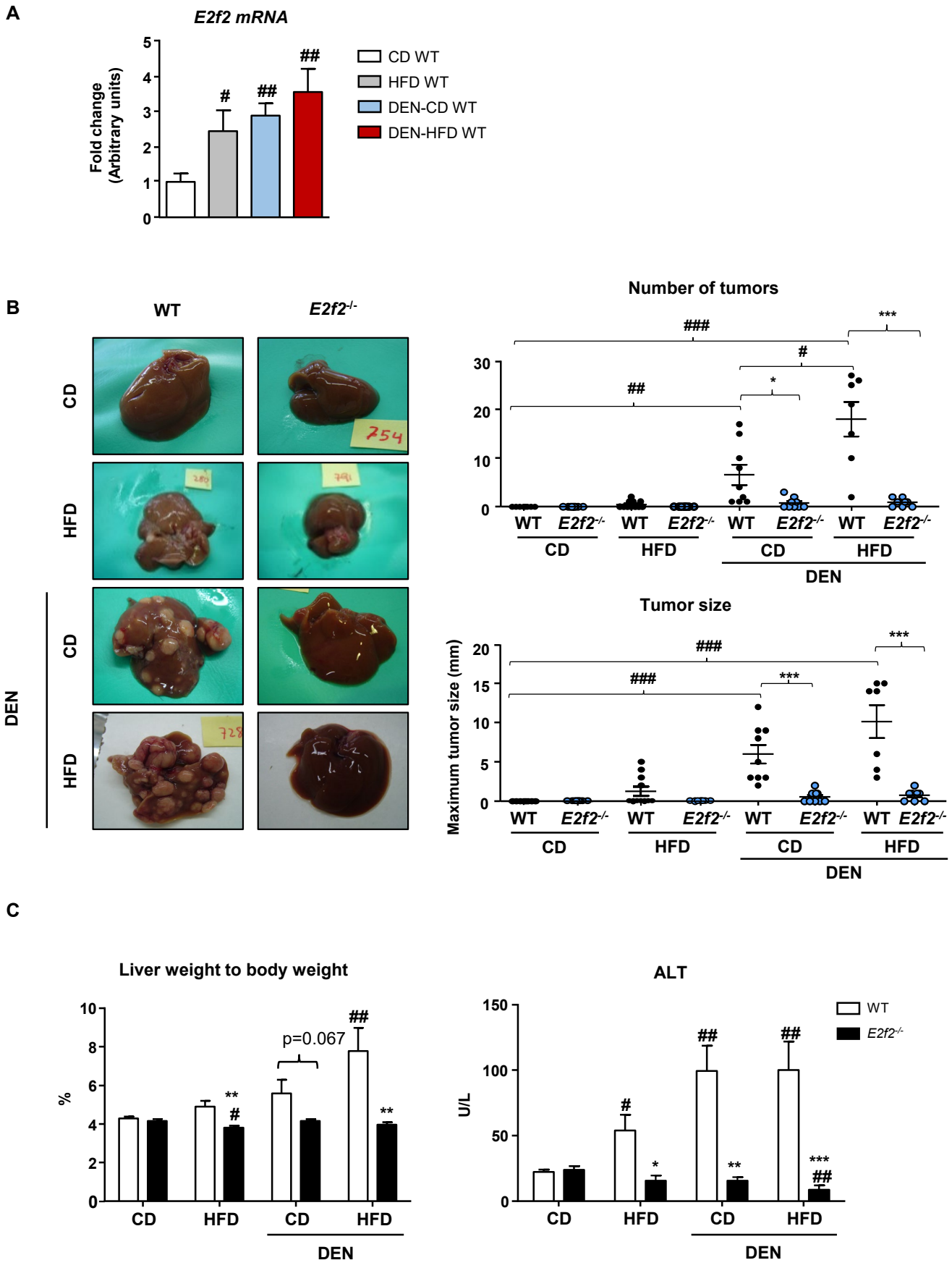
A
E2f2 mRNA
Fold change (Arbitrary units)
CD WT
HFD WT
DEN-CD WT
DEN-HFD WT
B
WT
E2f2-/-
CD
HFD
DEN
Number of tumors
Tumor size
Maximum tumor size (mm)
C
Liver weight to body weight
p=0.067
%
ALT
U/L

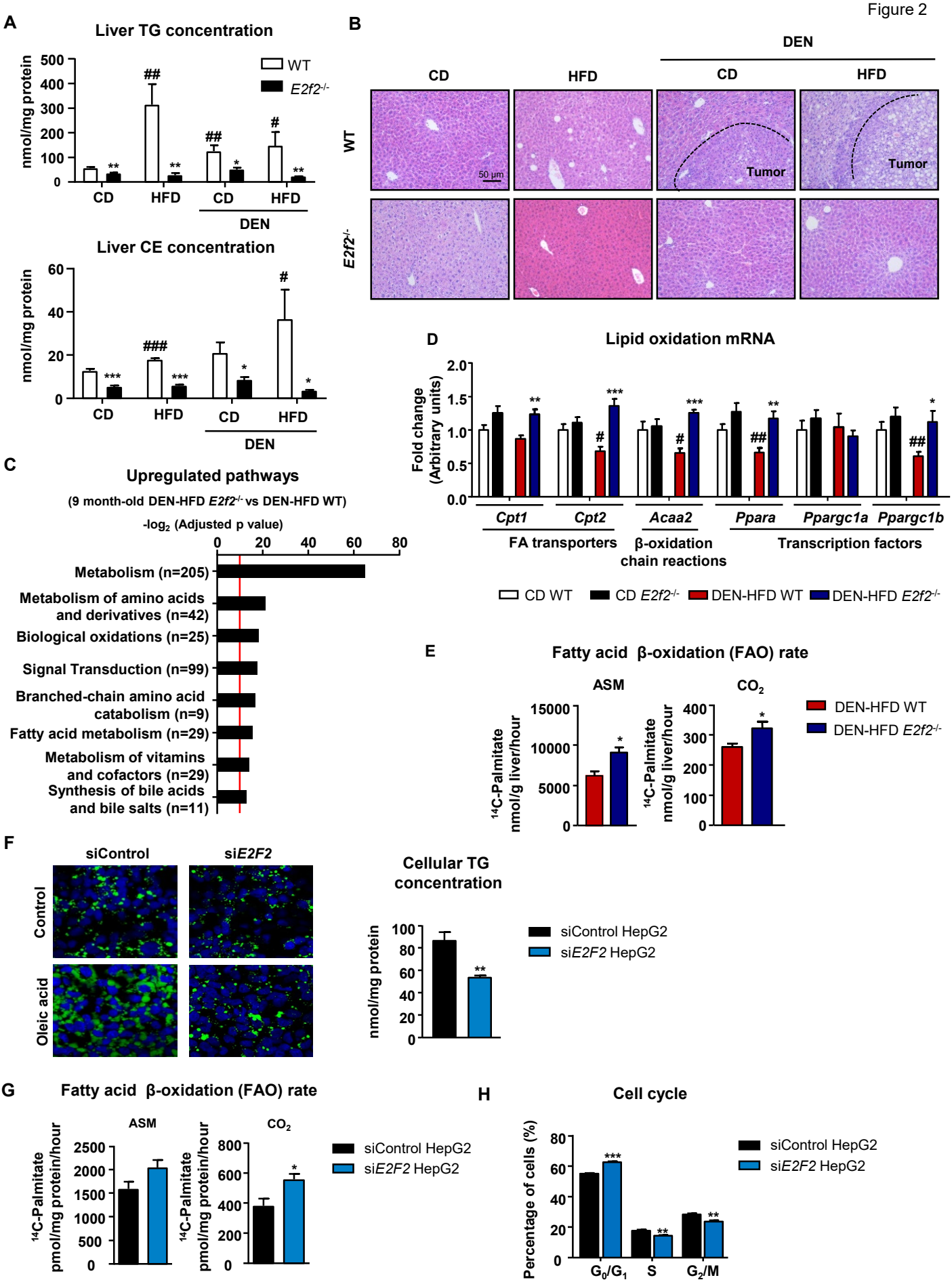
A
Liver TG concentration
nmol/mg protein
WT
E2f2-/-
CD
HFD
CD
HFD
DEN
Liver CE concentration
nmol/mg protein
CD
HFD
CD
HFD
DEN
B
DEN
CD
HFD
CD
HFD
WT
E2f2-/-
50 µm
Tumor
Tumor
C
Upregulated pathways
(9 month-old DEN-HFD E2f2-/- vs DEN-HFD WT)
-log2 (Adjusted p value)
Metabolism (n=205)
Metabolism of amino acids and derivatives (n=42)
Biological oxidations (n=25)
Signal Transduction (n=99)
Branched-chain amino acid catabolism (n=9)
Fatty acid metabolism (n=29)
Metabolism of vitamins and cofactors (n=29)
Synthesis of bile acids and bile salts (n=11)
D
Lipid oxidation mRNA
Fold change (Arbitrary units)
Cpt1
Cpt2
Acaa2
Ppara
Ppargc1a
Ppargc1b
FA transporters
β-oxidation chain reactions
Transcription factors
CD WT
CD E2f2-/-
DEN-HFD WT
DEN-HFD E2f2-/-
E
Fatty acid β-oxidation (FAO) rate
ASM
CO2
14C-Palmitate nmol/g liver/hour
DEN-HFD WT
DEN-HFD E2f2-/-
F
siControl
siE2F2
Control
Oleic acid
Cellular TG concentration
nmol/mg protein
siControl HepG2
siE2F2 HepG2
G
Fatty acid β-oxidation (FAO) rate
ASM
CO2
14C-Palmitate pmol/mg protein/hour
siControl HepG2
siE2F2 HepG2
H
Cell cycle
Percentage of cells (%)
G0/G1
S
G2/M
siControl HepG2
siE2F2 HepG2

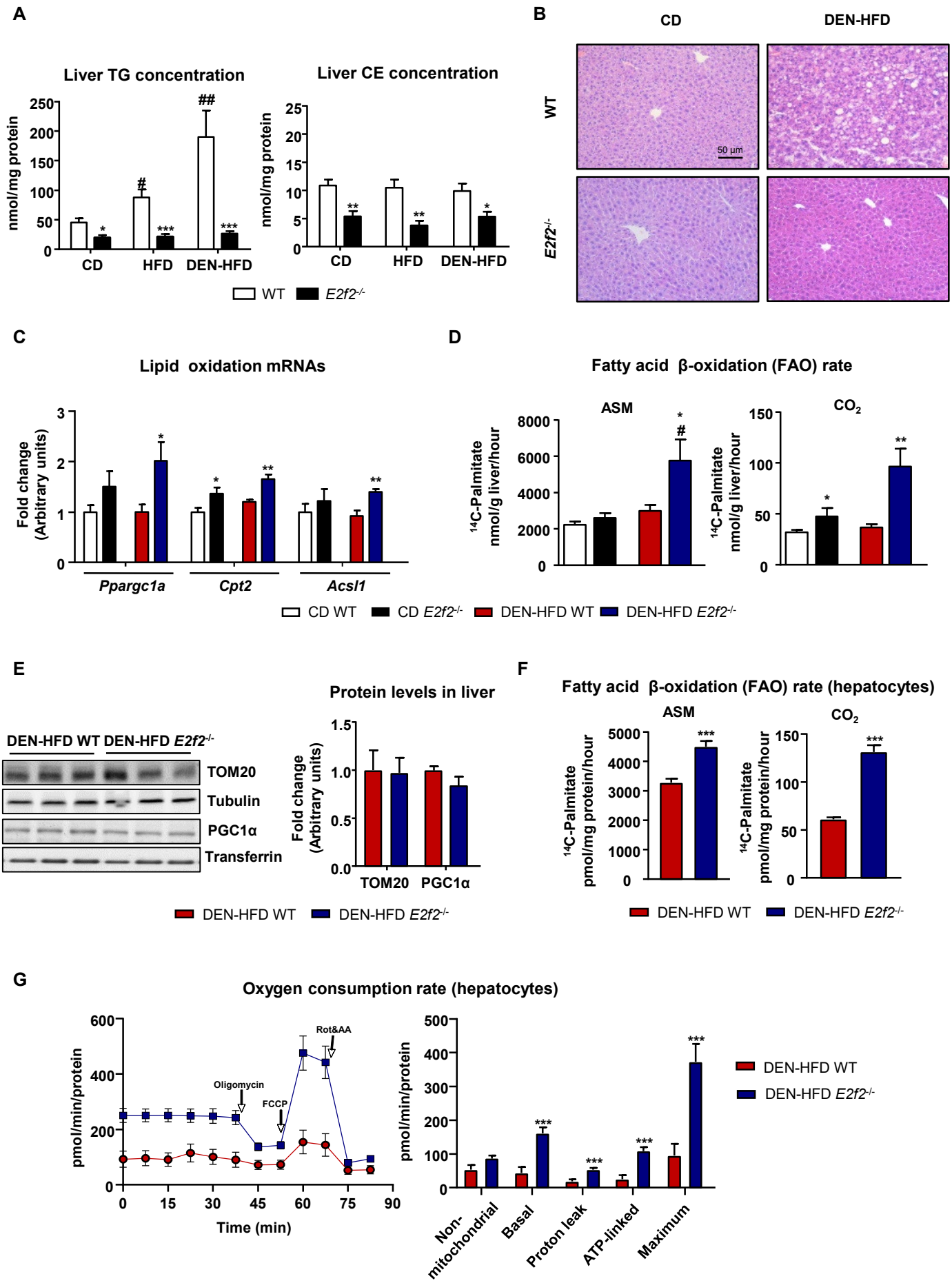
A
Liver TG concentration
nmol/mg protein
CD
HFD
DEN-HFD
Liver CE concentration
WT
E2f2-/-
B
CD
DEN-HFD
WT
E2f2-/-
50 μm
C
Lipid oxidation mRNAs
Fold change (Arbitrary units)
Ppargc1a
Cpt2
Acsl1
D
Fatty acid β-oxidation (FAO) rate
ASM
CO2
14C-Palmitate nmol/g liver/hour
CD WT
CD E2f2-/-
DEN-HFD WT
DEN-HFD E2f2-/-
E
DEN-HFD WT DEN-HFD E2f2-/-
TOM20
Tubulin
PGC1α
Transferrin
Protein levels in liver
Fold change (Arbitrary units)
TOM20
PGC1α
F
Fatty acid β-oxidation (FAO) rate (hepatocytes)
ASM
CO2
14C-Palmitate pmol/mg protein/hour
G
Oxygen consumption rate (hepatocytes)
pmol/min/protein
Oligomycin
FCCP
Rot&AA
Time (min)
Non-mitochondrial
Basal
Proton leak
ATP-linked
Maximum

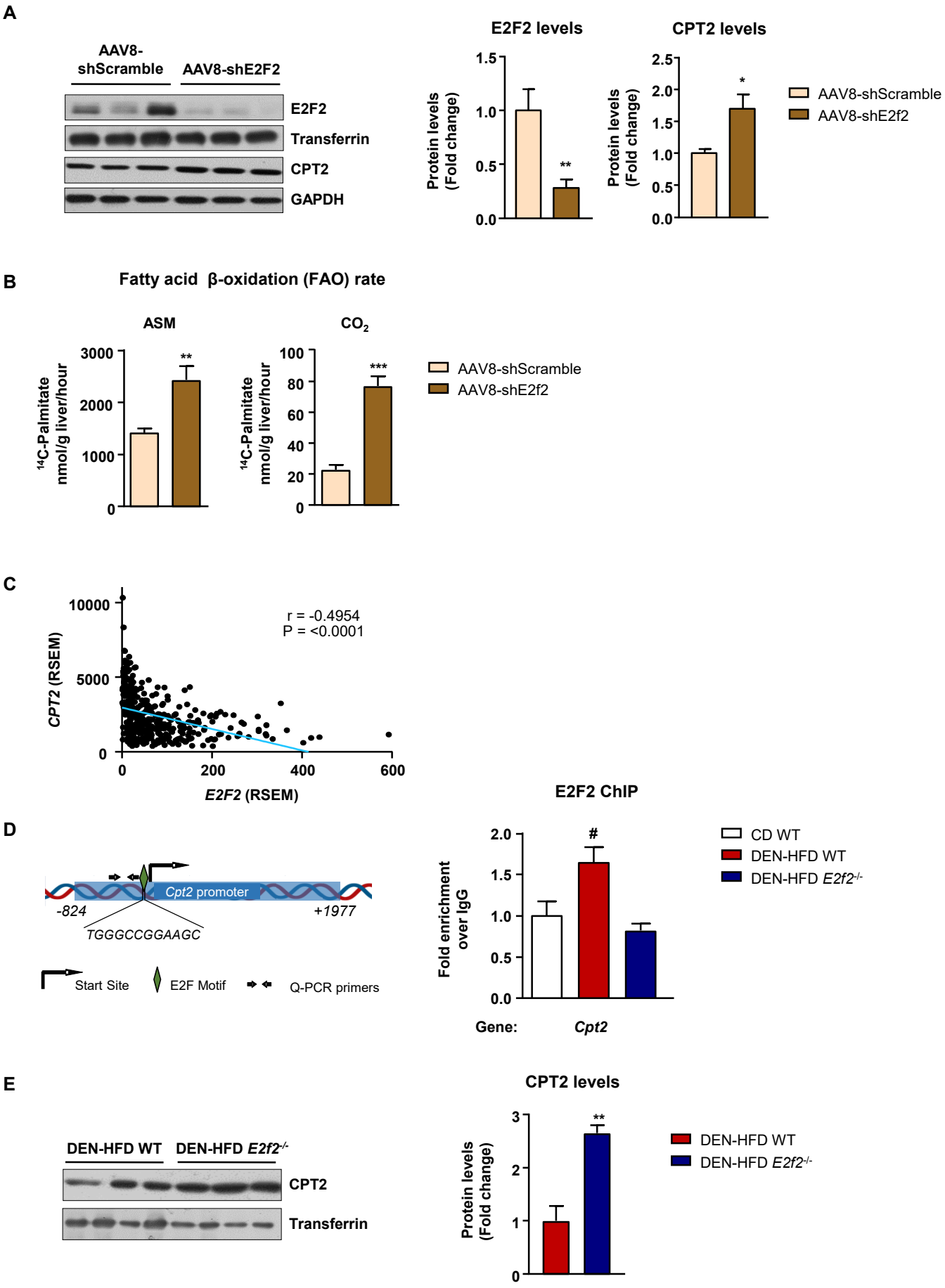
A
AAV8-shScramble
AAV8-shE2F2
E2F2
Transferrin
CPT2
GAPDH
E2F2 levels
CPT2 levels
Protein levels (Fold change)
AAV8-shScramble
AAV8-shE2f2
B
Fatty acid β-oxidation (FAO) rate
ASM
CO2
14C-Palmitate nmol/g liver/hour
C
CPT2 (RSEM)
E2F2 (RSEM)
r = -0.4954
P = <0.0001
D
Cpt2 promoter
-824
+1977
TGGGCCGGAAGC
Start Site
E2F Motif
Q-PCR primers
E2F2 ChIP
Fold enrichment over IgG
CD WT
DEN-HFD WT
DEN-HFD E2f2-/-
Gene:
Cpt2
E
DEN-HFD WT
DEN-HFD E2f2-/-
CPT2
Transferrin
CPT2 levels
Protein levels (Fold change)

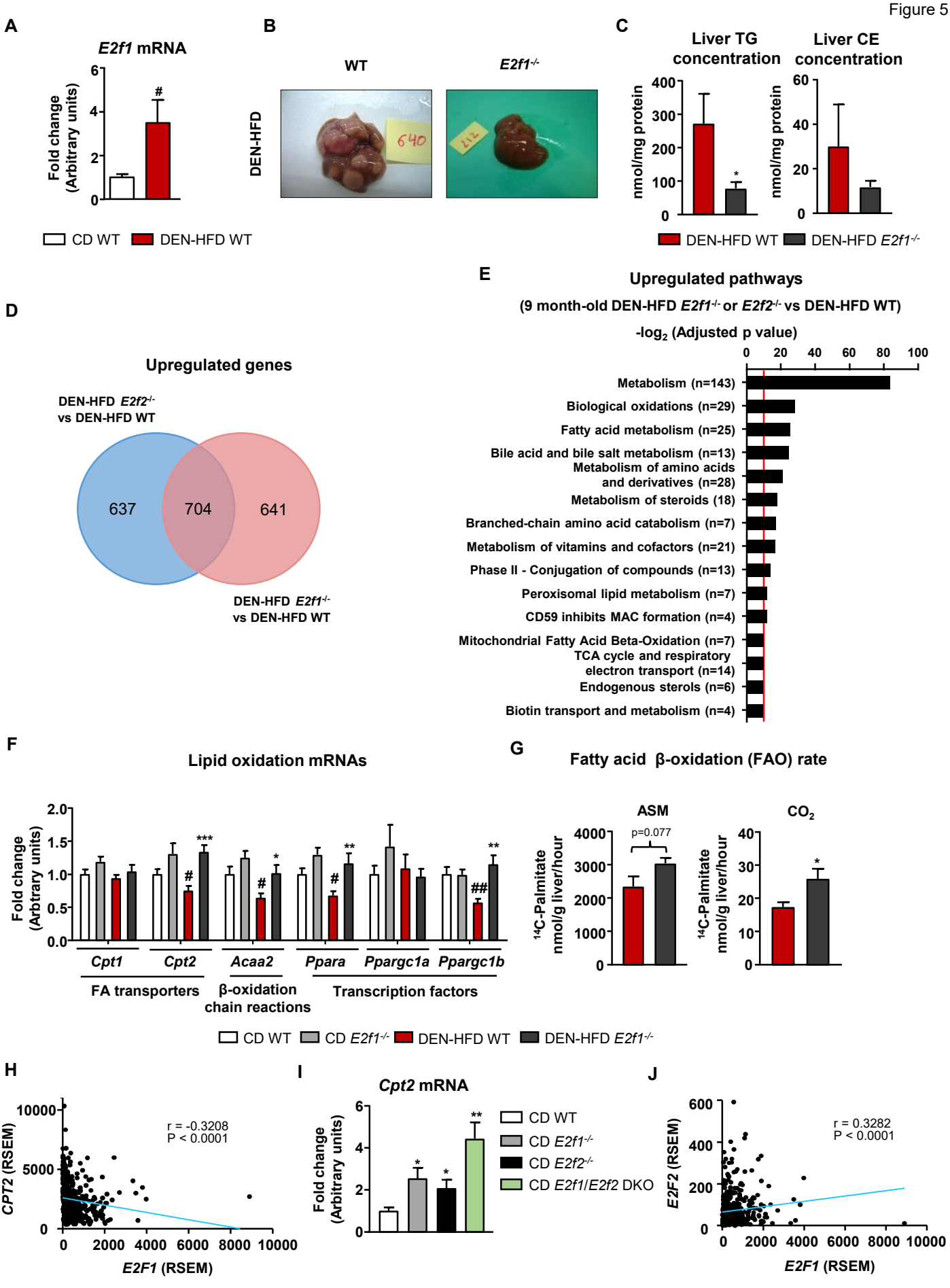
A
E2f1 mRNA
Fold change (Arbitrary units)
CD WT
DEN-HFD WT
B
WT
E2f1-/-
DEN-HFD
C
Liver TG concentration
Liver CE concentration
nmol/mg protein
DEN-HFD WT
DEN-HFD E2f1-/-
D
Upregulated genes
DEN-HFD E2f2-/- vs DEN-HFD WT
637
704
641
DEN-HFD E2f1-/- vs DEN-HFD WT
E
Upregulated pathways
(9 month-old DEN-HFD E2f1-/- or E2f2-/- vs DEN-HFD WT)
-log2 (Adjusted p value)
Metabolism (n=143)
Biological oxidations (n=29)
Fatty acid metabolism (n=25)
Bile acid and bile salt metabolism (n=13)
Metabolism of amino acids and derivatives (n=28)
Metabolism of steroids (18)
Branched-chain amino acid catabolism (n=7)
Metabolism of vitamins and cofactors (n=21)
Phase II - Conjugation of compounds (n=13)
Peroxisomal lipid metabolism (n=7)
CD59 inhibits MAC formation (n=4)
Mitochondrial Fatty Acid Beta-Oxidation (n=7)
TCA cycle and respiratory electron transport (n=14)
Endogenous sterols (n=6)
Biotin transport and metabolism (n=4)
F
Lipid oxidation mRNAs
Fold change (Arbtrary units)
Cpt1
Cpt2
Acaa2
Ppara
Ppargc1a
Ppargc1b
FA transporters
β-oxidation chain reactions
Transcription factors
G
Fatty acid β-oxidation (FAO) rate
ASM
CO2
p=0.077
14C-Palmitate nmol/g liver/hour
CD WT
CD E2f1-/-
DEN-HFD WT
DEN-HFD E2f1-/-
H
CPT2 (RSEM)
E2F1 (RSEM)
r = -0.3208
P < 0.0001
I
Cpt2 mRNA
Fold change (Arbitrary units)
CD WT
CD E2f1-/-
CD E2f2-/-
CD E2f1/E2f2 DKO
J
E2F2 (RSEM)
E2F1 (RSEM)
r = 0.3282
P < 0.0001

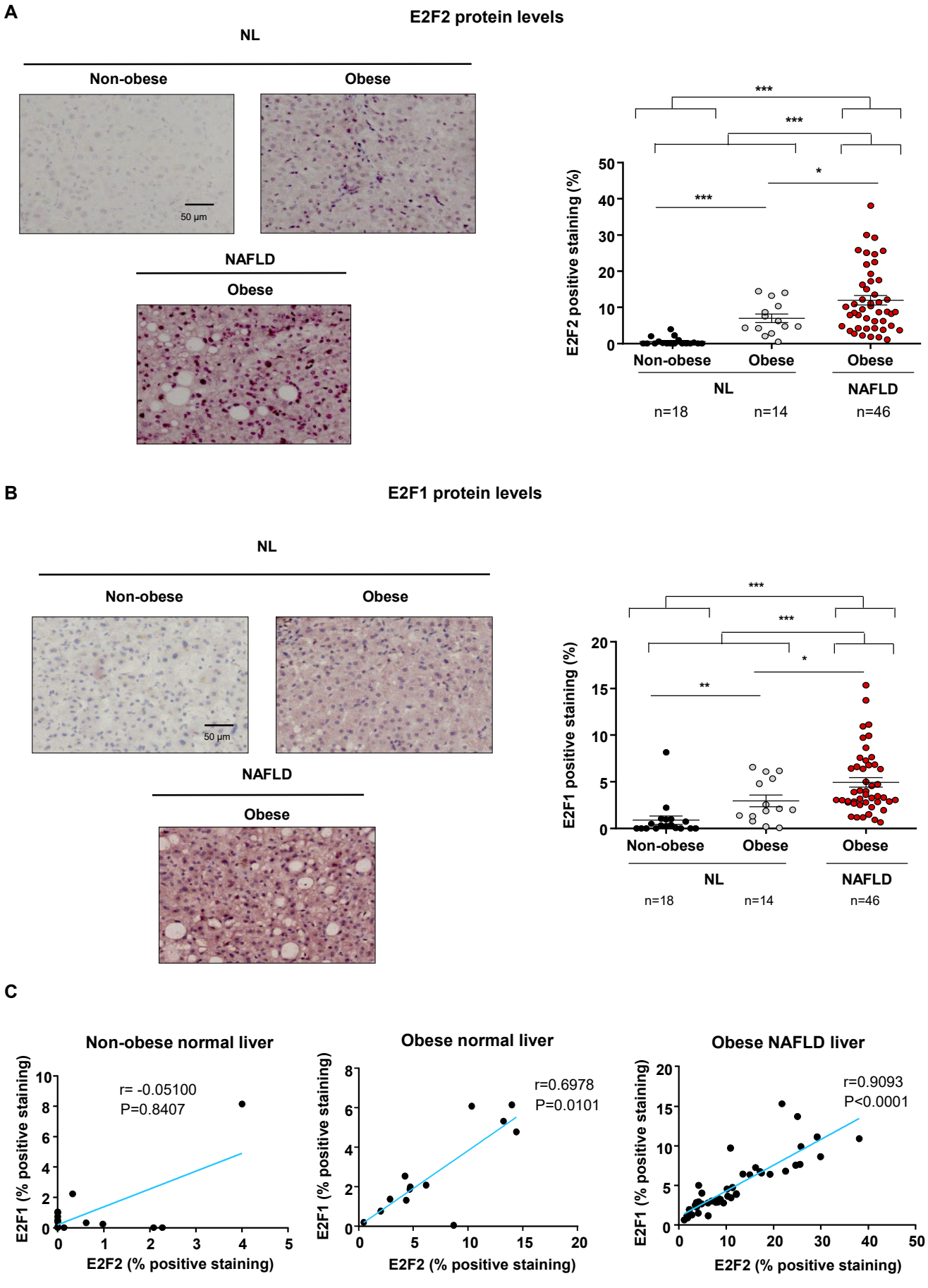
A
E2F2 protein levels
NL
Non-obese
Obese
50 µm
NAFLD
Obese
E2F2 positive staining (%)
Non-obese
Obese
Obese
NL
NAFLD
n=18
n=14
n=46
B
E2F1 protein levels
NL
Non-obese
Obese
50 µm
NAFLD
Obese
E2F1 positive staining (%)
Non-obese
Obese
Obese
NL
NAFLD
n=18
n=14
n=46
C
Non-obese normal liver
r= -0.05100
P=0.8407
E2F1 (% positive staining)
E2F2 (% positive staining)
Obese normal liver
r=0.6978
P=0.0101
E2F1 (% positive staining)
E2F2 (% positive staining)
Obese NAFLD liver
r=0.9093
P<0.0001
E2F1 (% positive staining)
E2F2 (% positive staining)

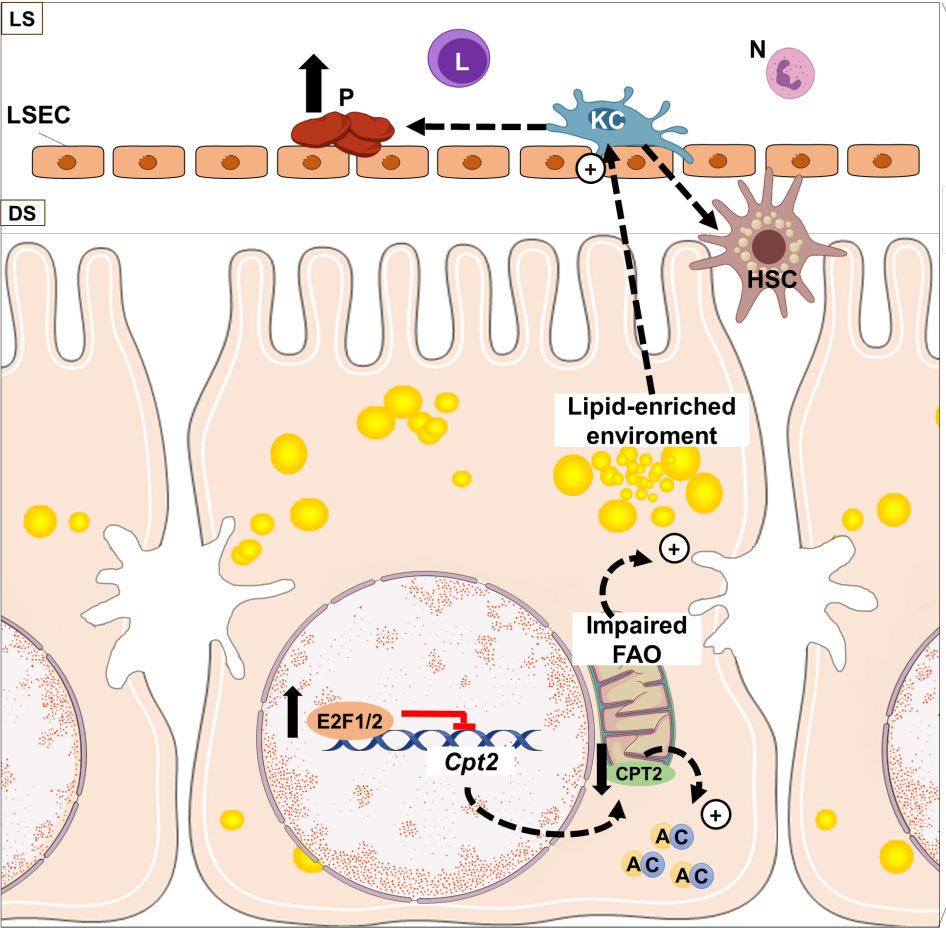

E2F1/2 in NAFLD development and progression to HCC

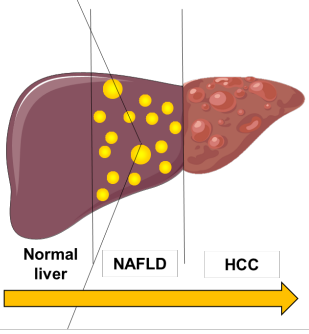

NAFLD progression to HCC

E2F1 and E2F2-mediated repression of CPT2 establishes a lipid-rich tumor-promoting environment

Francisco González-Romero[1,#], Daniela Mestre[1,2,#], Igor Aurrekoetxea[1,2], Colm J. O´Rourke[3], Jesper B. Andersen[3], Ashwin Woodhoo[4,5], Miguel Tamayo-Caro[4], Marta Varela-Rey[6], Marta Palomo-Irigoyen[4], Beatriz Gómez-Santos[1], Diego Sáenz de Urturi[1], Maitane Núñez-García[1], Juan L. García-Rodríguez[1], Larraitz Fernández-Ares[1,2], Xabier Buqué[1,2], Ainhoa Iglesias-Ara[7], Irantzu Bernales[8], Virginia Gutierrez De Juan[6], Teresa C. Delgado[6], Naroa Goikoetxea-Usandizaga[6], Richard Lee[9], Sanjay Bhanot[9], Igotz Delgado[1], Maria J. Perugorria[10,11], Gaizka Errazti[2], Lorena Mosteiro[2], Sonia Gaztambide[2,12], Idoia Martinez de la Piscina[2], Paula Iruzubieta[13], Javier Crespo[13], Jesus M. Banales[5,10], Maria L. Martínez-Chantar[6], Luis Castaño[2,12], Ana M. Zubiaga[7], Patricia Aspichueta[1,2,*]

[1]Department of Physiology, Faculty of Medicine and Nursing, University of Basque Country UPV/EHU, Leioa, Spain; [2]BioCruces Bizkaia Health Research Institute, Cruces University Hospital, CIBERehd, Barakaldo, Spain; [3]Biotech Research & Innovation Centre, Department of Health and Medical Sciences, University of Copenhagen, Denmark; [4]Center for Cooperative Research in Bioscience (CIC bioGUNE), Derio, Spain. [5]Ikerbasque, Basque Foundation for Science, Bilbao, Spain; [6]Liver Disease Laboratory, Center for Cooperative Research in Biosciences (CIC bioGUNE), Basque Research and Technology Alliance (BRTA), CIBERehd Derio, Spain; [7]Department of Genetic, Physical Anthropology and Animal Physiology, Faculty of Science and Technology, University of Basque Country UPV/EHU, Leioa, Spain; [8]SGIKER, University of Basque Country UPV/EHU, Leioa, Spain; [9]Ionis Pharmaceuticals, California, USA; [10]Department of Liver and Gastrointestinal Diseases, Biodonostia Health Research Institute, Donostia University Hospital, University of the Basque Country UPV/EHU, CIBERehd, San Sebastian, Spain; [11]Department of Medicine, Faculty of Medicine and Nursing, University of the Basque Country UPV/EHU, Leioa, Spain; [12]Faculty of Medicine and Nursing, University of Basque Country UPV/EHU, CIBERDEM, CIBERER. [13]Gastroenterology and Hepatology Department. Marqués de Valdecilla University Hospital. Santander, Spain.

[#]These authors contributed equally

***Corresponding author**: Patricia Aspichueta, Department of Physiology, Faculty of Medicine and Nursing, University of the Basque Country UPV/EHU, Barrio Sarriena s/n, 48940 Leioa, Spain. Phone: +34 946012896; Fax: +34 946015662; e-mail: patricia.aspichueta@ehu.eus

Running title: E2F1 and E2F2 promote NAFLD-related HCC

Keywords: CPT2/E2F/fatty acid oxidation/lipids/nonalcoholic fatty liver disease/hepatocarcinogenesis

Conflict of Interest: MLM-C is consultant of Mitotherapeutix. JMB reports grants from Incyte, personal fees for lecturer from Bayer and Intercept, and consulting for QED Therapeutics, Albireo Pharma and OWL Metabolomics, outside the submitted work. There are no other conflicts of interest.

Table of contents:

1. Supplementary material and methods

Human samples

This study comprised a total of 78 liver samples. Non-obese healthy human liver samples (NL) (n=18) were from donors who died from stroke (Marqués de Valdecilla University Hospital, Santander, Spain). Body mass index (BMI) in these donors was lower than 30 kg/m^2. Analysis of liver biopsies proved that livers were histologically normal and there was no evidence of hepatitis B virus (HBV), hepatitis C virus (HCV) and human immunodeficiency virus (HIV). Samples from obese patients (n=60) (Table S1) with a BMI higher than 30 kg/m^2 were obtained from liver biopsies with a diagnostic purpose (Cruces University Hospital, Barakaldo, Spain). Among these patients, 14 had histologically NL and 46 were diagnosed with non-alcoholic fatty liver disease (NAFLD) according to Kleiner's criteria (1). Inclusion criteria for obese patients were also based on the absence of alcohol (< 20 g per day) or potentially hepatotoxic drug intake. They showed negative serum tests for HBV, HCV and HIV. None of the patients suffered from autoimmune medical conditions. Written consent was obtained from each patient included in the study. The study was performed in agreement with the Declaration of Helsinki and with local and national laws. The Human Ethics Committee of each hospital and the University of Basque Country approved the study procedures and a written informed consent was obtained before inclusion in the study

E2F1 and *E2F2* expression analysis in TGCA-LIHC database

Level 3 RNA-seq and clinical datasets generated by TCGA-LIHC project (2) were downloaded from Firehose portal (Broad Institute). In total, 371 tumors and 50 surrounding normal tissues were analyzed). For correlation studies, data normality of genes expression values was assessed by D'Agostino & Pearson normality test. Subsequently, matched expression levels were evaluated by Spearman correlation.

Animals and housing conditions

Male *E2f2* knockout (*E2f2*$^{-/-}$), *E2f1* knockout (*E2f1*$^{-/-}$), *E2f1*/*E2f2* double knockout (DKO) and their wild type (WT) littermate mice (mixed background C57BL/6J and 129/Sv) were produced at the UPV/EHU animal facility. C57BL/6J mice (Jackson Laboratory, USA) were used for *E2f2* knockdown in the liver. The animals were housed in groups with an artificial 12 hours light (8:00 to 20:00)/12 hours dark cycle, under controlled temperature and humidity conditions and allowed free access to food and tap water. Animal procedures were approved by the Ethics Committee for Animal Welfare of the University of the Basque Country UPV/EHU, in accordance with the European Union Directives for animal experimentation.

HCC and NAFLD-related HCC were induced by an intraperitoneal injection of the hepatic carcinogen diethylnitrosamine (DEN) (25 mg/kg of mice, Sigma-Aldrich, USA) in 14 day-old *E2f2*$^{-/-}$ or *E2f1*$^{-/-}$ and WT mice (3). After weaning, at 1 month of age, mice were fed a high fat diet, DEN-HFD group, or a chow diet, (DEN-CD group) for 32 weeks and sacrificed at 9 months of age. Age-matched groups were administered vehicle alone (saline buffer) combined with HFD or CD.

For progressive NAFLD, administration of DEN was performed as described above and the HFD was administered for 10 weeks until mice were sacrificed at 3 months of age. Age-matched mice administered vehicle alone combined with HFD or CD were also included.

Liver-specific *E2f2* knock-down or overexpression was achieved in 2-month-old C57BL/6J mice fed a CD after infection with recombinant adeno-associated viruses serotype 8 (AAV8). Mice were sacrificed one month later. Specifically, the knockdown of *E2f2* in the liver was achieved by an intraperitoneal injection (a volume of 100 µl with 10^{10} PFU/mL) of *AAV8-EGFP-U6-mshE2F2* (named as AAV8-shE2F2); the control mice received an intraperitoneal injection of AAV8-shScramble. For *E2f2* overexpression, an intravenous injection (a volume of 100 µl with 10^{12} PFU/mL) of *AAV8-Alb-mE2F2* (named as AAV8-*E2f2*) was carried out. Mice injected with

AAV8-Alb-EGFP (named as AAV8-*Gfp*) were used as controls. Recombinant AAV8 vectors were obtained from Viral Vector Production Unit, Universitat Autònoma de Barcelona.

The *in vivo Creb* downregulation was performed with antisense oligonucleotides (ASO). For this, DEN-HFD *E2f2*$^{-/-}$ and WT mice were treated with an intraperitoneal injection of ASO CREB or ASO control (50 mg/kg of mice per week) (Ionis Pharmaceuticals, USA) during four weeks. Mice were sacrificed at 3 months of age**.**

Analysis of metabolic fluxes in animal models

Fatty acid β-oxidation rate

Fatty acid oxidation in liver homogenates was assessed as described before (4). Fresh liver pieces were homogenized in a Potter homogenizer (5 strokes) in cold buffer (25 mM Tris-HCl, 500 nM sucrose, 1 mM EDTA-Na_2 pH 7.4) and sonicated for 10 seconds. Then, the homogenates were centrifuged at 420 xg for 10 minutes at 4 ºC. Approximately 500 µg of protein from the homogenates supernatant was used for the assay in a volume of 60 µl. The reaction started by adding 340 µl of assay mixture (500 µM palmitate/0.4 µCi [1-^{14}C] palmitate (Perkin Elmer Inc, USA) per reaction) to the samples which were incubated with shaking for 30 minutes at 37 ºC in eppendorf tubes with a Whatman paper circle in the cap. The reaction was stopped by adding 200 µl of 1 M perchloric acid and 45 µl of 1 M NaOH was added to impregnate the Whatman cap. After 1 hour at room temperature, the Whatman caps were removed and the associated radioactivity was measured in a scintillation counter. The Eppendorf tubes were centrifuged at 21.000 xg 10 minutes at 4 ºC and 400 µl from the supernatant were collected and the radioactivity was counted in a scintillation counter. The supernatant contained the acid soluble metabolites (ASM) and the Whatman caps captured the released CO_2.

de novo lipogenesis of TG

de novo lipogenesis in tissue was performed as previously described (5) with slight modifications. Freshly isolated tissue slices (40 mg) were incubated in high glucose Dulbecco's Modified Eagle Medium (DMEM) with insulin (150 nM), 20 μM acetate and 20 μCi/ml [^{3}H]- acetic acid for 4 hours. Tissue slices were homogenized in saline buffer and lipids were extracted and quantified as described below.

Hepatic TG secretion rate

Hepatic TG secretion rate was measured *in vivo* in two-hour fasted mice treated with an intraperitoneal injection of Poloxamer P-407. TG concentration was measured immediately prior to injection and 6 hours following injection with a commercial kit (A. Menarini Diagnostics, Italy).

Tissue and serum extraction

Unless otherwise specified, mice were fasted for 4 hours and subsequently euthanized with sodium pentobarbital (Abbott Laboratories, Spain) injected intraperitoneally (60 mg/kg of mice). Tissues were collected and washed in cold PBS and rapidly weighed. If applicable, tumors in liver were counted and measured with a caliper. Next, tissues were sliced immediately into several pieces to be used in metabolic assays and fixed with formalin (Sigma-Aldrich, USA) or OCT (Tissue-Tek® O.C.T. Compound, Sakura® Finetek) for histological analysis or to be frozen in liquid nitrogen and stored at -80 °C for biochemical analyses. Blood was drawn and allowed to clot at room temperature for 30 minutes. Next, the serum was obtained after two centrifugations: the first one at 2,000 xg for 30 minutes at 4°C and the second one at 10,000 xg for 10 minutes at 4°C.

HepG2 cell line culture

For each experiment, a new aliquot of newly bought human hepatoma cell line HepG2 (ATCC, USA) was acquired. Cells were cultured in maintenance medium (1 g/L glucose containing Eagle's minimum essential medium (EMEM), ATCC, USA) supplemented with 100 IU/ml penicillin, 100 µg/ml streptomycin, 2 mM L-glutamine and 10 % (v/v) fetal bovine serum (FBS) at 37 °C and 5 % CO_2 and were used with a maximum of 5-6 passages.

***E2F2* knock-down in HepG2 cell line**

Knock-down experiments were performed by reverse transfection of siRNA oligonucleotides. Pre-designed E2F2-specific siRNA (si*E2F2)* (#4392420, from Ambion, USA) and non-target negative control siRNA (siControl) (Ambion, USA) were used. Lyophilized siRNAs were resuspended in nuclease-free sterile water at 50 mM and the stock solutions were stored at -20 °C. Work solutions were prepared for immediate use at 1 mM. siRNA (final concentration 12 nM for western blot and 18 nM for lipid and metabolic fluxes assays), OptiMEM Reduced Serum (Gibco, USA) and RNAiMAX lipofectamine (Invitrogen Life Technologies, USA) were incubated in the culture dishes for 20 minutes at room temperature. Afterwards, HepG2 cells resuspended in gene silencing medium (1 g/L glucose containing EMEM supplemented with 2 mM L- glutamine and 10 % (v/v) FBS) were added to siRNA-containing dishes and cultured for 48 hours.

***E2F2* overexpression in HepG2 cell line**

Overexpression experiments were performed by reverse transfection with the mammalian expression plasmid pRc-CMV-HA-E2FpE2F2 (p*E2F2*) and its empty vector control.

Plasmid transfection was performed with 2.5 ug of DNA per well in 6-well plates as explained above for gene knock-down. Briefly, OptiMEM Reduced Serum (Gibco, USA), plasmid and RNAiMAX lipofectamine (Invitrogen Life Technologies, USA) were incubated in the culture dishes for 20 minutes at room temperature. Afterwards, HepG2 cells resuspended in gene transfection medium (1 g/L glucose containing EMEM supplemented with 2 mM L- glutamine and 10 % (v/v) FBS) were added to plasmid-containing dishes and cultured for 24 hours.

Cell cycle analysis

HepG2 cells were cultured in Dulbecco's modified Eagle medium (DMEM) containing 10% FBS and supplemented with antibiotics (100 units of penicillin/ml and 100 µg/ml of streptomycin) at 37°C in a humidified atmosphere containing 5% CO_2. The cells were transfected with siControl or si*E2F2* RNAs and synchronized in G_2/M with nocodazole (250 ng/ml nocodazole (Sigma) 24 hours post-transfection). After 24 h of treatment with nocodazole, cells were washed and released from the G_2/M cell cycle arrest. 24 h later the cells were washed twice with ice-cold phosphate-buffered saline (PBS), fixed in 70% cold ethanol for 1 h, and labeled with 5 µg/mL propidium iodide (PI) containing 250 µg/mL ribonuclease A (Roche) for 1 h at room temperature. Cells were analyzed by flow cytometry.

Primary mouse hepatocyte isolation, culture and gene overexpression and silencing

For experiments with hepatocytes, primary cells were isolated from mixed background C57BL/6J and 129/Sv WT and *E2f2*$^{-/-}$. Livers were washed by perfusion with carbogenated Krebs-Henseleit (KH) medium supplemented with Ca_2^+, and with carbogenated KH medium supplemented with 0.05% (w/v) ethyleneglycoltetraacetic acid (EGTA) (Sigma-Aldrich; USA) successively. Then, an enzymatic digestion was performed with carbogenated KH supplemented with 300 µg/ml collagenase type A and 60 µg/ml trypsin inhibitor (Roche; Switzerland). After perfusion and digestion, livers were mechanically disaggregated and cells were washed with complete media.

Isolated viable hepatocytes were seeded over collagen and fibronectin-coated culture dishes for cell adhesion. Cells were finally cultured at 37 °C in a humidified atmosphere of 5% CO_2.

Overexpression of *E2f2* in primary hepatocytes was achieved by infection with adenovirus (VectorBuilder) expressing *E2f2* (Ad-*E2f2*) for 1.5 hours and harvesting 36 hours post-treatment. Adenovirus expressing GFP was used as control.

For *Rb* knock-down in primary hepatocytes, predesigned Rb-specific siRNA (siRB) was used (#4390824, Ambion, USA) was used to a final concentration of 0.2 μM. DharmaFECT was used as transfection reagent (Horizon, United Kingdom). Hepatocytes were treated with siRNAs for 12 hours and harvested 48 hours post-treatment.

Seahorse analysis in primary mouse hepatocytes

Glycolysis. Mouse hepatocytes were isolated and glycolysis experiments were performed as previously described (6). Briefly, hepatocytes were seeded onto Seahorse XF24 cell culture microplates (Seahorse Bioscience) at 20000 cells per well in complete media. After 4 hours of attachment, hepatocytes were glucose starved overnight. Cells were then washed and placed in an unbuffered DMEM–based medium containing 2 mM glutamine for 1.5 hours. Next, glucose 25 mM was injected into the cells directly with the Seahorse apparatus and ECAR measurement was performed. The normalized data were expressed as mpH per minute, per amount of protein.

Oxygen Consumption Rate (OCR). OCR of primary mouse hepatocytes was measured at 37ºC by high resolution respirometry, with the Seahorse Bioscience XF24-3 Extracellular Flux Analyzer. Primary mouse hepatocytes were cultured onto XF24 cell culture microplates (Seahorse Bioscience) at 20000 cells per well in complete media. After 4 hours of attachment, cells were washed and new complete media was added overnight. Next day, cell culture media was replaced by new media of MEM without bicarbonate containing 10 mM sodium pyruvate, 10 mM glutamine and 1X non-essential amino acids. Cells were then placed on a CO_2 free incubator, at 37ªC, for at least one hour. Meanwhile, the XF assay cartridge (Seahorse Bioscience) was

prepared. Pharmacologic inhibitors were used with the following final concentration: oligomycin 1 mM, an inhibitor of ATP synthase; carbonyl cyanide 4-trifluoromethoxyphenylhydrazone (FCCP) 0.3 mM, an uncoupling agent that allows maximum electron transport, and Rotenone 0.5 mM/Antimycin 0.5 mM mix for inhibition of mitochondrial respiration. Once the cartridge was ready, cells were placed within the Seahorse Bioscience XF24 and upon the sequential delivery of the inhibitors, changes in the OCR were measured. The normalized data were expressed as pmol of O_2 per minute, per amount of protein quantified by crystal violet staining.

Analysis of fatty acid β-oxidation rate in cell cultures

Fatty acid oxidation rate in cells cultures was performed as follows. HepG2 cells were first incubated in pre-treatment media (EMEM, 1 % glutamine, 0.5 % BSA fatty acid free, 1 g/L glucose and 1mM oleic acid) for 24 hours followed by a 4 hours incubation with 0.2 mM palmitate containing 0.5 µCi/ml [^{14}C]-palmitate (Perkin Elmer Inc, USA) in low glucose medium. For primary hepatocytes, cells were incubated for 12 hours in pre-treatment media (DMEM, 1 % glutamine, 0.5 % BSA fatty acid free, 1 g/L glucose) followed by a 4 hour incubation as with HepG2 cells. Culture medium was collected in a tube containing Whatman filter paper soaked with 0.1 M NaOH in the cap and 500 µl of 1 M perchloric acid were added to the medium. Samples were incubated during one hour at room temperature. The acidified medium was centrifuged at 21000 xg for 10 minutes to remove particulate matter. The radioactivity of CO_2 captured by the filter papers and the radioactivity in acid-soluble metabolites (the supernatants of the culture media) was measured by a scintillation counter**.**

Cytochemistry of neutral lipids

Sterilized circular coverslips were used to seed 7.5x10^4 cells. Then, cells were washed three times with saline buffer and were fixed with formaldehyde 3.7 % (v/v) (Panreac, Spain). For cell permeabilization, sample was incubated in 0.25 % (v/v) Triton (Sigma-Aldrich, USA) in saline

buffer for 5 minutes at room temperature. Afterwards, three washes were performed and cells were blocked with 10% (v/v) FBS (Biochrom, UK) for 15 minutes. Neutral lipid droplets were stained with BODIPY 493/503 green lipophilic fluorescent dye (1:200) (Invitrogen Life Technologies, USA) for 2 hours. Subsequently, coverslips were washed 3 times in order to remove the remaining dye and cell nuclei were incubated with DAPI blue fluorescent probe (Sigma-Aldrich, USA) (1:1000 in PBS) for 5 minutes. All the steps were carried out at room temperature. Finally, coverslips were mounted with aqueous mounting media (Dako, Denmark). Optical images were taken with Olympus Fluoviwe FV500 confocal microscopy in the SGIker Microscopy Service from the UPV/EHU.

Quantification of lipids

Pieces of livers (30 mg) were homogenized in 10 volumes of ice-cold saline buffer in a Potter homogenizer (20 strokes). For quantification in HepG2 cells, $1.5x10^6$ cells were directly scraped in 1 ml of distilled H_2O. In both cases, lipids were extracted from 1.5 mg of protein (7), separated by thin layer chromatography (TLC) and quantified as described (8). For total quantification of CE in tissue, TLC plates were stained with a solution of 10 % $CuSO_4$ (w/v) in 8% H_3PO_4 (v/v) and an image of the plate was digitalized with GS-800 densitometer (Bio-Rad Laboratories, USA). Quantification was performed with Quantity One software (Bio-Rad Laboratories, USA). A part of the lipid extract was also dissolved in isopropanol (Scharlau Chemicals, Spain) and TGs were measured with a commercial kit (A. Menarini Diagnostics; Ripolli, Italy) following manufacturer´s protocol.

Quantification of ALT

ALT was measured in serum obtained from the inferior vena cava of mice with a commercial colorimetric method following the manufacturer's instructions (Spinreact, Spain).

Malonyl Coenzyme A determination

Quantitative determination of endogenous mouse malonyl coenzyme A concentrations in tissue homogenates was assessed with a commercial ELISA kit following the manufacturer's instructions (MyBiosource USA).

RNA isolation and quantitative real-time polymerase chain reaction (RT-qPCR)

Total RNA was isolated by using Trizol Reagent (Invitrogen; Carlsbad, CA, USA) according to the manufacturer's protocol (RNA was precipitated with chloroform and isopropanol, washed with 80% ethanol, and finally dissolved in RNase-free water). For liver samples, 30 mg of tissue were homogenized in 1 ml of Trizol Reagent with Polytron PT 1200 homogenizer in an ice bath for 30 seconds. For cellular samples, cells were directly scraped in 1 ml of Trizol Reagent. In both cases, 1.8 μg of total RNA extracted was subjected to DNase treatment (Invitrogen, USA) and cDNA synthesis was performed with SuperScript III First-Strand Synthesis System for RT- PCR kit (Invitrogen, USA) following the manufacturer's protocol. First strand cDNA was synthesized in the presence of random primers and RNase OUT to prevent RNA contamination in the sample. RT-qPCR was performed in the SGIker Genomic Service from the UPV/EHU, using the BioMark HD system in combination with Dynamic Array Integrated Fluidic Circuits (IFC) (Fluidigm Corporation, USA). The protocol used was Fluidigm's Fast Gene Expression Analysis using EvaGreen on the BioMark HD System version D1. Target and reference genes were specifically preamplified with Multiplex PCR Master (Qiagen, Netherlands) (95 ˚C 15 minutes, 14 cycles of 95 ˚C for 15 seconds and 60 °C for 4 minutes). 50 nM of primers were used. Afterwards, remaining primers were removed with Exo I (Thermo Scientific, USA) following the manufacturer instructions. Samples were diluted 1:5 with 0.1 mM EDTA containing TE buffer and were loaded onto 96.96 Dynamic Array IFC. SsoFastTM EvaGreen® Supermix with Low ROX (Bio-Rad, USA) was used for amplification. GE Fast 96x96 PCR + Melt v2 protocol was followed for PCR. All genes were run in duplicate. Finally, the stability of candidate reference

genes for normalization was assessed with NormFinder and GeNorm algorithms (9) using GenEx software (MultiD 5.2 version). For mice samples, glyceraldehyde- 3-phosphate dehydrogenase (Gapdh), cyclophilin A (Ppia), TATA box binding protein (Tbp) and actin (Actb) expression were used to calculate the normalization factor. Primers sequences are described in Table S2.

Microarray analysis

Microarray data have been deposited in NCBI's Gene Expression Omnibus (GEO) database and are accessible through accession number GSE117420.

Firstly, RNA integrity was assessed on an Agilent 2100 Bioanalyzer with Agilent RNA 6000 Nano chips (Agilent Technologies, USA). RNA samples were labeled and hybridized following standard Protocol "One-Color Microarray-Based Gene Expression analysis (Low Input Quick Amp Labeling)" Version 6.5 (Agilent Technologies, USA). In brief, 50 ng of total RNA were retrotranscribed with AffinityScript Reverse Transcriptase (Agilent Technologies, USA), using Oligo dT primers coupled to T7 promoter. Double stranded cDNA synthesized by AffinityScript RT was in vitro transcribed by T7 RNA pol in the presence of Cy3-CTP to generate amplified and labeled cRNA. Labeled samples were then purified with silica-based RNeasy spin columns (Qiagen, Germany). Yield and specific activity of each reaction was determined by quantifying the cRNA in the NanoDrop 1000 spectrophotometer. A sample was considered valid when yield was > 0.825 µg and specific activity was 3-6 pmol/µg.

Samples were then analyzed using Agilent SurePrint G3 Mouse GE 8x60 K microarrays (Design ID 028005) (Agilent Technologies, USA), in which 55,681 mouse features are represented. 600 ng of labeled cRNA samples were hybridized at 65 °C for 20 hours. Arrays were scanned on a G2565CA DNA microarray scanner and images were processed using Agilent Feature Extraction Software (vs. 10.7.3.1). Default parameters for one-color gene expression microarrays were used for image analysis, data extraction, background correction, and flagging of non-uniform features, population outliers in replicated features and with no significant intensities in Cy3 channel. Raw

data from Feature Extraction software was subsequently processed on GeneSpring GX 12.5 (Agilent Technologies, USA). Data were normalized by quantile normalization and mean centering. Data with non-uniform features, population outliers or features whose intensities were not significantly above the background signal in all samples of 1 out of any 4 conditions were excluded from the analysis. Differential gene expression between both mice strains was analyzed with LIMMA statistical package using MultiExperiment Viewer (MeV) vs. 4.7.1 (http://www.tm4.org/mev/) application. A multi-class comparison has been done. The adjusted p-values (adj-p-value) were obtained applying Benjamini-Hochberg method (False discovery rate, FDR) for multiple test correction. Genes with and adj-p-values < 0.05 in the comparisons of interest have been selected for further functional Analysis. To assess the biological relevance of each list, pathway enrichment analysis was performed using the ClueGO (v2.3.3) application, a plugin of the Cytoscape platform (http://www.cytoscape.org, v3.4.0). Reactome (http://www.reactome.org) pathway database was used for gene biological assessment. Enriched term selection was based on the Benjamini-Hochberg corrected p-value (Right-sided hypergeometric test) < 0.05 criterion.

Chromatin immunoprecipitation

For chromatin immunoprecipitation (ChIP) analyses in liver, 30 mg of the tissue were first homogenized in saline buffer with a Dounce homogenizer. The tissue solution was crosslinked by addition of formaldehyde to 1% final concentration. In case of cells, hepatocytes were directly crosslinked on the culture plate. Crosslinking proceeded at room temperature for 7 minutes and was stopped with glycine to 0.125 M final concentration. Cell pellets were collected by centrifugation of the tissue solution or the cell suspension and they were lysed on ice for 10 minutes with a cell lysis buffer containing 20 mM Tris-HCl pH 8.0, 85 mM KCl, 0.5% NP-40, and 1X of protease inhibitor cocktail (Roche). Nuclei were collected by centrifugation and disaggregated with a Dounce Homogenizer in Nuclear lysis buffer containing 10 mM Tris-Cl pH 8.0, 1 mM EDTA, 1% SDS and 1X protease inhibitor cocktail. Nuclei solution was finally

incubated for 10 minutes on ice. Chromatin was sonicated on a Diagenode Bioruptor to an average length of 200–500 bp. After microcentrifugation, the supernatant was diluted 10-fold in ChIP dilution buffer (0.01% SDS, 1.1% Triton X-100, 1.1 mM EDTA, 20 mM Tris-Cl pH 8.0, and 167 mM NaCl). Inmunoprecipitation of crosslinked-Protein/DNA was achieved by using protein G magnetic beads (ThermoFischer, pre-washed with saline buffer/1%BSA) which were incubated at 4°C for 3 hours in a rotation mixer with E2F2 (Santa Cruz, sc-9967) as antibody of interest and normal mouse IgG (BD Pharmingen, 557273) as negative control. Next, samples were incubated with magnetic beads-antibody at 4° C overnight with rotation. Protein G bead-antibody/chromatin complexes were recovered and washed once with Low Salt Wash Buffer (20 mM Tris-Cl pH 8.0, 0.1% SDS, 1% Triton X-100, 2 mM EDTA, 150 mM NaCl), High Salt Wash Buffer (20 mM Tris-Cl pH 8.0, 0.1% SDS, 1% Triton X-100, 2 mM EDTA, 500 mM NaCl), LiCl Wash Buffer (10 mM Tris-Cl pH 8.0, 0.25 M LiCl, 1% IGEPAL, 1% Na- deoxycholate, 1 mM EDTA) and finally with TE buffer. The elution of the complexes was carried out with a buffer containing 100mM $NaHCO_3$ and 1% SDS. Crosslinking was reversed by addition of NaCl to a final concentration of 200 mM in addition to use a buffer for RNA removing and protein digestion (250 mM Tris-HCl pH 6.5, 62.5 mM EDTA pH 8.0, 5 mg/ml Proteinase K and 62.5 µg/ml RNase A) followed by an overnight incubation at 65°C. After cooling the samples down, beads were separated using a magnet.

The DNA was extracted and purified with Quiagen QIAquick PCR purification kit. Quantification of immunoprecipitate-enriched DNA sequences was performed by real-time PCR or Fluidigm system as described below. PCR primers were designed considering the INSECT 2.0 predicted binding sites for E2F2 in the regulatory region of genes of interest. Primers sequences are detailed in Table S2**.**

Western blotting

The liver tissue was homogenized with the corresponding homogenization buffer (10 mM NaF, 1% (v/v) NP-40, 2 mM Na_3VO_4, 150 mM NaCl, 50 mM 4-(2-hydroxyethyl)-1-piperazineethanesulfonic acid (HEPES), 10 % (v/v) glycerol (Merck-Millipore, Germany), 10 mM $Na_4P_2O_7$, 2 mM EDTA-Na_2, 2 mM phenylmethanesulfonyl fluoride (PMSF), 0.1 mM leupeptin (Fisher Scientific, USA), pH 7.4). The protein concentration was determined in supernatants by a commercially available Bicinchoninic Acid (BCA) Reagent (ThermoFisher Scientific, USA) following manufacturer´s protocol. Next, the protein lysates were subjected to SDS-PAGE and PageRuler Plus Protein Ladder (ThermoFisher Scientific, USA) was used as molecular weight marker. The separated proteins were transferred and immobilized onto nitrocellulose membranes (AmershamTM ProtranTM, 0.2 µm, GE HealthCare, UK) by wet eletroblotting using Mini Trans-Blot cell (Bio-Rad, USA). Membranes were then blocked with blocking buffer for 1 hour at room temperature and incubated with commercial primary antibody overnight at 4 °C. Next day, membranes were incubated in 5 % (w/v) BSA in TBST containing secondary antibody conjugated to horseradish peroxidase (HRP) for 1 hour at room temperature. Immunoreactive proteins were detected by ECL Western blotting detection chemiluminiscence Reagent (GE Healthcare, UK) and exposed to RX-N X-Ray film (Fujifilm, Japan). Subsequently, the film was developed and fixed with photography liquids (AGFA, Belgium). For quantification, Quantity One software (Bio-Rad) was used and the antibodies that were used are detailed in Table S3.

Hematoxylin and eosin staining

Liver pieces were fixed in 10% (v/v) non-buffered formalin (Sigma-Aldrich, USA) for 24 hours at 4 °C and were kept in 50% (v/v) ethanol (Scharlau Chemicals, Spain) until they were paraffinized. The paraffin blocks were prepared and cut in 5 µm-thick sections with the microtome. They were picked up in poly-lysine treated microscope slides (Thermo Scientific,

USA) and fixed overnight at 37 °C. Paraffin embedded section was deparaffinized in xylene (Sigma-Aldrich, USA), rehydrated with decreasing ethanol solutions (Scharlau Chemicals, Spain) and washed with distilled water (dH_2O). After that, it was stained with ShandonTM Harris Hematoxylin (Thermo Scientific, USA) for 2.5 minutes and washed with dH_2O. Sample was decolorized by immersion in 0.5% (v/v) HCl (Merck-Millipore, Germany) and washed with dH_2O. Then, tissue was counterstained with Eosin-Y Alcoholic (Thermo Scientific, USA) for 25 seconds, washed and dehydrated with increasing ethanol solutions. Finally, samples were mounted using DPX mounting medium (Sigma-Aldrich, USA). Representative micrographs were taken under 20x from upright optical microscope.

2. Supplementary references

1. Kleiner DE, Brunt EM, Van Natta M, Behling C, Contos MJ, Cummings OW, et al. Design and validation of a histological scoring system for nonalcoholic fatty liver disease. *Hepatology*. 2005;41(6):1313-1321.

2. Comprehensive and integrative genomic characterization of hepatocellular carcinoma. *Cell*. 2017;169(7):1327-1341.e23.

3. Park EJ, Lee JH, Yu G, He G, Ali SR, Holzer RG, et al. Dietary and genetic obesity promote liver inflammation and tumorigenesis by enhancing IL-6 and TNF expression. *Cell*. 2010;140(2):197-208.

4. Huynh FK, Green MF, Koves TR, Hirschey MD. Measurement of fatty acid oxidation rates in animal tissues and cell lines. *Meth Enzymol*. 2014;542:391-405.

5. Nassir F, Adewole OL, Brunt EM, Abumrad NA. CD36 deletion reduces VLDL secretion, modulates liver prostaglandins, and exacerbates hepatic steatosis in ob/ob mice. *Journal of lipid research*. 2013;54(11):2988.

6. Denechaud P, Lopez-Mejia IC, Giralt A, Lai Q, Blanchet E, Delacuisine B, et al. E2F1 mediates sustained lipogenesis and contributes to hepatic steatosis. *Journal of Clinical Investigation*. 2016;126(1):137.

7. Folch J, Lees M, Sloane Stanley GH. A simple method for the isolation and purification of total lipides from animal tissues. *J Biol Chem*. 1957;226(1):497-509.

8. Ruiz JI, Ochoa B. Quantification in the subnanomolar range of phospholipids and neutral lipids by monodimensional thin-layer chromatography and image analysis. *J Lipid Res*. 1997;38(7):1482-1489.

9. De Spiegelaere W, Dern-Wieloch J, Weigel R, Schumacher V, Schorle H, Nettersheim D, et al. Reference gene validation for RT-qPCR, a note on different available software packages. *PLoS ONE*. 2015;10(3):e0122515

3. Supplementary figure legends

Figure S1. E2F2 expression is increased in human HCC. (A) Analysis of *E2F2* expression in HCC patients. *E2F2* expression was evaluated in different tumor and disease stages in TCGA-LIHC cohort. (B) Schematic representation of NAFLD-driven HCC induction in mice. (C) E2F2 protein levels in WT and *E2f2*$^{-/-}$ mice (n=7). (D) Mice were treated for 32 weeks to induce hepatocarcinogenesis and were sacrificed at 9 months of age. Hepatic mRNA levels of genes involved in cell cycle progression (n=6-8 per group). (E) Mice were fed a high fat diet for 32 weeks and were sacrificed at 9 months of age. Hepatic mRNA levels of genes involved in cell cycle progression in HFD treated livers (n=7-10 per group). For human samples analysis, data normality was evaluated by D'Agostino-Pearson omnibus test. Subsequent group-based comparisons of non-normal data were performed using Mann-Whitney U test. Significance was defined as *p<0.05, **p <0.01 and **p <0.001. For mouse studies, values represent mean ± SEM. Significant differences between CD and DEN-HFD are denoted as #p <0.05, ##p <0.01, and ###p

<0.001. (Student's t test). Differences between WT and *E2f2*$^{-/-}$ are indicated by *p <0.05, **p <0.01 and ***p <0.001 (Student's t test). CD, chow diet; HFD, high fat diet; DEN, diethylnitrosamine; HCC, hepatocellular carcinoma; SL, surrounding liver; RSEM, RNA-seq by expectation maximization.

Figure S2. Transcriptomic signature in 9-month-old DEN-HFD treated *E2f2*$^{-/-}$ mice. Mice were treated for 32 weeks to induce hepatocarcinogenesis and were sacrificed at 9 months of age. (A) RNA was extracted from liver homogenates and a gene expression microarray analysis was carried out (n=4 mice per group). Differential gene expression between both genotypes was analyzed and significant probes were assigned into pathways with Reactome database. Biological pathways including downregulated genes ($p \leq 0.001$) in DEN-HFD *E2f2*$^{-/-}$ mice vs DEN-HFD WT mice are shown ($-\log_2$ of 0.001 is indicated with a red line). (B) Hepatic mRNA levels of genes involved in lipid oxidation and oxidative phosphorylation (n=7-8 mice per group). (C) WT and *E2f2*$^{-/-}$ mice were fed a high fat diet for 30 weeks and were sacrificed at 9 months of age. Fatty acid β-oxidation rate was determined in liver by measuring the amount of [^{14}C]-CO_2 and [^{14}C]-ASM (n=6 mice per group). (D) Hepatic mRNA levels of genes involved in lipid oxidation and oxidative phosphorylation in HFD fed mice (n=7-10 mice per group). (E) Heatmap showing relative expression of genes involved in cell cycle and metabolism in CD, HFD and DEN-HFD 9-month-old WT and *E2f2*$^{-/-}$ mice. All data are relative to the CD WT group values. The statistical study of differences was performed in each genotype between the HFD and the CD group (1) and between the DEN-HFD and the HFD group (2). Heatmaps were generated using GraphPad Prism 8. Values represent mean ± SEM and statistical analysis was determined by Student's two-tailed t-test. Significant differences between *E2f2*$^{-/-}$ and WT mice, p*E2F2* and pCMV or siControl vs si*E2F2* are denoted as *p <0.05, **p <0.01 and ***p <0.001. Differences between DEN-HFD and CD are denoted as $^{\#}$p <0.05, $^{\#\#}$p <0.01 and $^{\#\#\#}$p <0.001. CD, chow diet; HFD, high fat diet; DEN, diethylnitrosamine; ASM, acid soluble metabolites; NS, non-significant.

Figure S3. **E2F2 overexpression in liver induces fatty acid oxidation but does not alter mRNA levels of cell cycle genes.** (A) Confirmation of *E2F2* after knock-down (*siE2F2*) and overexpression (*pE2F2*) in HepG2 cell line (n=6 per group). (B) Fatty acid β-oxidation rate was determined in cells by measuring the amount of [^{14}C]-CO_2 and [^{14}C]-ASM (n=5 per group). (C) mRNA levels of *MCM3* in HepG2 cells transfected with p*E2F2* compared to their controls (n=5-6 per group) (left) and cell cycle distribution analysis in these cells (n=8 per group) (right). (D) *in vivo* E2F2 overexpression in the liver was achieved by injection of recombinant AAV8-*E2f2* in mice. Confirmatory overexpression of E2F2 at the protein and mRNA levels is shown (n=4 mice per group). (E) Fatty acid β-oxidation rate was determined in liver by measuring the amount of [^{14}C]-CO_2 and [^{14}C]-ASM (n=4-5 mice per group). (F) Hepatic mRNA levels of genes involved cell cycle (n=4 mice per group). Values represent mean ± SEM. Statistical analysis was determined by Student's two-tailed t-test. Significant differences between AAV8-*Gfp* and AAV8-*E2f2* are denoted as *p <0.05, **p <0.01 and ***p <0.001. AAV8; Adeno associated virus serotype 8; ASM, acid soluble metabolites.

Figure S4. Loss of *E2f2* protects liver from inflammation and ER stress. Mice were treated with DEN and fed a high fat diet for 10 weeks and were sacrificed at 3 months of age. (A) Hepatic mRNA levels of genes involved in cell cycle regulation (n=5-8 mice per group). (B) Ki67 immunostaining analysis (n=5-7 mice per group). Representative images of *E2f2*$^{-/-}$ and WT mice livers are shown. (C) ALT analysis in liver homogenates (n=6-8 mice per group) and liver to body weight ratio (n=9 mice per group). (D) Hepatic mRNA levels of genes involved in inflammation (n=7-8 mice per group). (E) Western blot analysis of the main proteins involved in endoplasmic reticulum stress in liver (n=6 mice per group). Values represent mean ± SEM. Significant differences between CD and DEN-HFD are denoted as #p <0.05, ##p <0.01, and ###p <0.001. (Student's t test). Differences between WT and *E2f2*$^{-/-}$ are denoted as by *p <0.05, **p <0.01 and ***p <0.001 (Student's t test). CD, chow diet; HFD, high fat diet; DEN, diethylnitrosamine.

Figure S5. E2F2 regulates fatty acid β-oxidation rate in liver. Mice were treated with DEN and fed a high fat diet for 10 weeks and were sacrificed at 3 months of age. (A) Hepatic mRNA levels of genes involved in lipid oxidation (n=7-8 mice per group). (B) Hepatic mRNA levels of genes implicated in oxidative phosphorylation (n=7-8 mice per group). (C) Mice were fed a high fat diet for 10 weeks and subsequently sacrificed at 3 months of age. Hepatic mRNA levels of genes involved in lipid oxidation (n=7-8 mice per group). (D) Hepatic mRNA levels of genes involved in oxidative phosphorylation (n=7-8 mice per group). (E) Fatty acid β-oxidation rate was determined in liver by measuring the amount of [^{14}C]-CO_2 and [^{14}C]-ASM (n=4-5 mice per group). (F) Oxygen consumption rate (OCR) in hepatocytes was measured using the Seahorse analyzer (n=11-12 per group) Values represent mean ± SEM. Significant differences between CD and DEN-HFD are denoted as #p <0.05, ##p <0.01, and ###p <0.001. (Student's t test). Differences between WT and *E2f2*$^{-/-}$ are denoted as *p <0.05, **p <0.01 and ***p <0.001 (Student's t test). CD, chow diet; HFD, high fat diet; DEN, diethylnitrosamine; ASM, acid soluble metabolites.

Figure S6. E2F2 does not regulate glycolysis or *de novo* lipogenesis in DEN-HFD treated mouse livers. Mice were treated with DEN and fed a high fat diet for 10 weeks and were sacrificed at 3 months of age. (A) Extracellular acidification rate (ECAR) was determined after glucose treatment in primary cultures of hepatocytes isolated from chow diet fed mice using a Seahorse analyzer (n=6 per group). (B) ECAR was determined after glucose treatment using a Seahorse analyzer in primary cultures of hepatocytes isolated from DEN-HFD treated mice (n=11-12 per group). (C) Hepatic mRNA levels of glycolysis rate-limiting genes (n=6-8 mice per group). (D) Hepatic mRNA levels of genes involved in *de novo* lipogenesis (n=6-8 mice per group). (E) Malonyl-CoA levels in liver (n=6-7 mice per group). (F) *de novo* lipogenesis of TG was quantified by the amount of [^{3}H]-acetate incorporated into TG (n=5 mice per group). (G) Hepatic mRNA levels of genes involved in VLDL metabolism (n=7-8 mice per group). (H) Hepatic TG secretion rate (n=5 mice per group). Values represent mean ± SEM and statistical analysis was determined by Student's two-tailed t-test. Significant differences between DEN-

HFD and CD are determined by $^{\#}p < 0.05$, $^{\#\#}p < 0.01$ and $^{\#\#\#}p < 0.001$. Differences between *E2f2*$^{-/-}$ and WT mice are denoted as $^{*}p < 0.05$, $^{**}p < 0.01$ and $^{***}p < 0.001$. CD, chow diet; HFD, high fat diet; DEN, diethylnitrosamine; TG, triglyceride; VLDL, very-low density lipoprotein.

Figure S7. E2F2 does not regulate *de novo* lipogenesis or VLDL secretion in HFD fed mouse livers. Mice were fed a high fat diet (HFD) for 10 weeks and were sacrificed at 3 months of age. (A) Hepatic mRNA levels of genes involved in *de novo* lipogenesis (n=7-8 mice per group). (B) *de novo* lipogenesis of TG was quantified by the amount of [^{3}H]-acetate incorporated into TG (n=4-5 mice per group). (C) Hepatic mRNA levels of genes involved in VLDL metabolism (n=7-8 mice per group). (D) Hepatic TG secretion rate (n=3-4 mice per group). Values represent mean ± SEM and statistical analysis was determined by Student's two-tailed t-test. Significant differences between *E2f2*$^{-/-}$ and WT mice are denoted as $^{*}p < 0.05$, $^{**}p < 0.01$ and $^{***}p < 0.001$; HFD, high fat diet; TG, triglyceride; ASM, acid soluble metabolites; VLDL, very-low density lipoprotein.

Figure S8. Analysis of E2F2 enrichment in promoters of metabolism-regulating genes by chromatin immunoprecipitation (ChIP). E2F2 overexpression in cultured primary hepatocytes was achieved through the infection of an adenovirus carrying *E2f2* gene (Ad-*E2f2).* (A) Confirmation of E2F2 overexpression at the protein and mRNA levels (n=6 per group). (B) mRNA levels of *Cpt2* upon Ad-*E2f2* treatment (n=6 per group). (C) Analysis of E2F2 binding activity to promoters of genes related to fatty acid metabolism (n=4 per group). (D) Analysis of E2F2 binding activity to promoters of genes related to glycolysis (n=4 per group). (n=4 per group). (E) Analysis of E2F2 binding activity to promoters of genes related to mitochondrial function (n=4 per group). Values represent mean ± SEM and statistical analysis was determined by Student's two-tailed t-test. Significant differences between Ad-*Gfp* and ad-*E2f2* are denoted as $^{*}p < 0.05$, $^{**}p < 0.01$ and $^{***}p < 0.001$.

Figure S9. CREB cooperated with E2F2 in the regulation of *Cpt2*. (A) *Rb* knock-down was carried out in primary hepatocytes using siRNA transfection. Confirmation of RB knock-down at the protein and mRNA levels (n=6 per group). (B) *Cpt2* mRNA levels after *Rb* knock-down in hepatocytes derived from DEN-HFD WT (n=5 per group) or CD WT mice (n=6 per group). (C) Predicted CREB binding site in the promoter of *CPT2* according to Ensembl Genome Browser. (D) Mice were treated for 10 weeks to induce liver disease and subsequently sacrificed at 3 months of age. Liver CREB1 and CPT2 protein levels (n=4-6 mice per group) in DEN-HFD WT mice treated with ASOs (left). Fatty acid β-oxidation rate was determined by measuring the amount of [^{14}C]-CO_2 and [^{14}C]-ASM in liver homogenates of DEN-HFD WT mice treated with ASOs (n=4-6) (right). (E) Liver CREB1 and CPT2 protein levels (n=5-8 mice per group) in DEN-HFD *E2f2*$^{-/-}$ mice treated with ASOs (left). Fatty acid β-oxidation rate was determined by measuring the amount of [^{14}C]-CO_2 and [^{14}C]-ASM in liver homogenates of DEN-HFD *E2f2*$^{-/-}$ mice treated with ASOs (n=5-6 mice per group) (right). Values represent mean ± SEM. Significant differences between Control ASO and CREB ASO or siControl and si*Rb* are denoted as *p <0.05, **p <0.01 and ***p <0.001 (Student's t test). CD, chow diet; HFD, high fat diet; DEN, diethylnitrosamine; ASM, acid soluble metabolites; ASO, anti-sense oligonucleotide.

Figure S10. E2F1 deficiency leads to an increased expression of genes involved in lipid oxidation in mice. (A) Analysis of *E2F1* expression in HCC patients. *E2F1* expression was evaluated in different tumor and disease stages in TCGA-LIHC cohort. (B) Mice were treated for 32 weeks to induce hepatocarcinogenesis and subsequently sacrificed at 9 months of age. RNA was extracted from liver homogenates and a microarray analysis was carried out (n=4 mice per group). Differential gene expression between *E2f1*$^{-/-}$ and WT was analyzed and significant probes were assigned into pathways with Reactome database. Biological pathways including upregulated genes (p ≤0.001) in mice are shown (–$\log_2$ of 0.001 is indicated with a red line). (C) Biological pathways including downregulated genes (p ≤0.001) in mice are shown (–$\log_2$ of 0.001 is indicated with a red line). (D) Hepatic mRNA levels of genes involved in oxidative phosphorylation lipid oxidation in 9-month-old mice (n=7-8 mice per group). (E) Hepatic mRNA

levels of genes implicated in lipid oxidation (n=7-8 mice per group) in 9-month-old mice. (F) *E2f1* mRNA levels in 3 month-old *E2f2*$^{-/-}$ mouse livers (n=4-8 mice per group). (G) *E2f1* mRNA levels in 9 month-old *E2f2*$^{-/-}$ mouse livers (n=4-8 mice per group). For human samples analysis, data normality was evaluated by D'Agostino-Pearson omnibus test. Subsequent group- based comparisons of non-normal data were performed using Mann-Whitney U test. Significance was defined as *p<0.05, **p <0.01 and **p <0.001. For mice studies, values represent mean ± SEM. Significant differences between CD and DEN-HFD are denoted as #p <0.05, ##p<0.01, and ###p <0.001. (Student's t test). Differences between WT and *E2f2*$^{-/-}$ are denoted as *p <0.05, **p <0.01 and ***p <0.001 (Student's t test). CD, chow diet; HFD, high fat diet; DEN, diethylnitrosamine; HCC, hepatocellular carcinoma; SL, surrounding liver; RSEM, RNA-seq by expectation maximization.